KHAZAR UNIVERSITY

Faculty: Engineering and Applied Sciences

Department: Computer Sciences

Specialty: Informatics

MASTER THESIS

Theme: Technological Innovation in Banking and Payments

Master Student: Aytakin Nabisoy

Supervisor: Ph.D. Mahammad Sharifov

BAKU – 2017

Contents

Abstract

This thesis describes how the latest technological innovations rebuild the banking system, creating new products and services, increasing access for consumers, strengthening banking management systems and cutting costs. At the same time, technological innovation also changes existing business models, increasing competition, squeezing margins and changing the nature of interaction with customers. By collecting these opportunities, banks, regulators and politicians can create a more secure and efficient banking system that can meet the needs of customers and parties in the digital age.

New technologies and the pace of innovation reorganize banking business models and working models, and also affect the shape and dynamics of a wider ecosystem of financial services. Early users of new technologies gain a significant advantage over competitors. Other banks may choose a more coherent approach for strategic purposes - to postpone adoption of new technologies until they are proved by competitors.

Introduction

Associated with the fast development of information and communication technology (ICT), the modes of operations in banking sector has been changed from on-side to remote and upgraded to telephone banking, and quickly entered into the era of online-banking. At present, it has been moving towards the development of generation of M-banking (mobile banking).To ensure security, M-banking has assimilated, a smart card, a one-time password (OTP), a user-defined password, as a method of risk of breaking into M-banking services. In the previous version, OTP was used to send an OTP message to a personal mobile phone, but now M-banking can easily be implemented by most smartphones. Therefore, there is a higher risk to information security due to mobile phone hacking. The personal biometrics such as finger, face and iris have been admitted and connected with the OTP for the verification of M-banking. Client defined OTP message is generated at the server side and it is sent to the mobile phone via internet. Now the user is assumed to enter the OTP received via a webpage of the M-banking system for the purpose of verification gain authority to perform further next transactions.

With the progress of large scale network such as social network, e-commerce, e-learning and growing concern of theft personal information, the design of secure personal authenticationsystem is important. Usually, person authentication for applications like access control to a restricted area, or for identification in different networks or social services scenarios, is done using biometric systems. A biometric system is explained as “a system which automatically differentiate and recognizes a person as individual and unique through a combination of hardware and pattern recognition algorithms based on certain physiological or behavioral characteristics that are specific to that person. Biometric characteristics are divided into two parts: physiological characteristics and behavioral characteristics. Some characteristics that are used for biometric recognition include face, fingerprint, hand-geometry, ear, iris, retina, DNA, palm print, hand vein etc. are physiological characteristics. In biometric recognition systems,behavioral characteristics are defined by voice, gait, signature, keystroke dynamics.Any behavioral or physiological attribute may qualify for a biometric test if it does not meet criteria such as (a) universality: possesses all people; (B) distinctiveness: discriminatory among the population; C) Invariance: the selected biometric feature should exhibit (D) collection: easily collected from the point of view of acquiring, digitizing and isolating characteristics from the population, (e)

efficiency: refers to the availability of resources and imposition of real restrictions in terms of data collection and guaranteeing the achievement of high Accuracy, (f) acceptability: the willingness of the public to present this attribute to the recognition system.

Chapter 1 Digital Banking

1.1 Technological Innovations

Banks are undergoing a fundamental transformation as a result of improved technological innovation. Currently, six technologies are most popular in the field of financial innovation: cloud computing, large data and analytics, AI, machine learning (ML), automation of robotics (RPA) processes, distributed accounting technology (DLT) and Internet of things. These technologies are at different stages of maturity, and some of them can significantly change the industry in later years.

Cloud computing

Cloud computing is an Internet model for the provision of information technology (IT) services. It allows you to centrally combine IT resources, quickly deliver and quickly reallocate resources. Banks are strengthening cloud computing to address the limitations of scaling the legacy infrastructure and ensuring cost-effectiveness of access to advanced technologies developed by other service providers. Early adoption of cloud technologies was focused on infrastructure and software services based on suppliers. Despite this, the use of cloud technologies to improve business functions and the main functions of the front office took more slowly to minimize data security, confidentiality and operational risk.

Big data and analytics

In particular, big data refers to technologies that allow the acquisition, collection and analysis of large amounts of data - whether structured, multi-structured (for example, sensor data) or unstructured (e.g. text, e-mail, video). Analytics refers to the detection, clarification and transmission of significant patterns in the data. These technologies are supported by a number of integrated disciplines, including applied statistics and mathematics, operations research and computer programming. However, earlier and more advanced uses of analytics for forecasting trends and prescriptive actions in areas such as risk management are in the early stages of adoption.

Artificial intelligence/machine learning.

Artificial Intelligent (AI) machine learning (ML) allows computers to learn from data for the purpose of predicting and / or solving outside the human scale. Artificial intelligence is a form of expanded analytics that tries to imitate human nature, like learning, understanding complex meaning, developing special conclusions and using in a natural dialogue. AI can replicate human cognitive abilities (for example, cognitive calculations) or increase and improve human performance when performing non-standard tasks. At present, this technology is being introduced purposefully throughout the financial services industry, primarily in the areas of risk and compliance, such as trade supervision.

Machine learning is a type of artificial intelligence that automates the construction of analytical models, allowing computers to learn without explicit development under the impact of new data. Machine learning consists of two different methods, controlled and uncontrolled. In controlled learning, there are two variables: input (x) and output (y). And using the algorithm to study the mapping function from the input to the output: Y = f (X). In a controlled learning process, an algorithm learning from a set of learning materials. We know that the correct goal corresponds to an algorithm that makes predictions iteratively on the learning data and is corrected by the teacher. When the algorithm reaches an acceptable level of performance, training stops.

Unsupervised learning identifies patterns from the data without hinting at the target result, such as fraud detection.

Robotic process automation(RPA)

RPA refers to the automation of repetitive processes to collect and explain existing tools for transaction processing, data management, response, or data exchange with other digital systems. Any company that makes extensive use of the workforce for routine work, where people perform high-performance, high-performance process functions, will support their capabilities and save money and time with the automation software of the robotic process.

Distributed ledger technology

Often called "block chain" technology, DLT is a shared database distributed over a network (individuals, organizations or devices), in which a list of hearings between participants grows. Transactional recording is synchronized, since each copy of the

record is the same and is automatically updated and unchanged, since the data written in the register cannot be changed. The development of intelligent contacts (for example, business logic built into a distributed register) has introduced a new dimension of functionality. Banks are currently evaluating a distributed ledger and intelligent contact technology for various uses, including master data management, issuance and maintenance of assets / securities, collateral management and trade / contact verification.

Internet of Things

Internet Things (IoT) is a network of sensors connected to the Internet that can be connected to physical devices (things). These devices can collect data and share it over the Internet with people, applications and other devices. This allows you to measure and monitor the behavior and other properties of people and things. IoT is widely distributed in industries with physical products (for example, telephones, cars, electrical recycling) and services (for example, internal security services of health services). Nevertheless, IoT banks are still at an early stage, and the adopters focus on how (ı) we increase these financial services related to other industries (for example, mobile banks and payments), and (ii) apply it to the digital product and the development of services.

1.2 Digital-era in banking system

a) Historically, the banking industry has developed both together and as a result of broad political, economic, legal / regulatory, social and technological forces. Although the recent financial crisis and reforms continue to play an important role in broader changes in the structure and operational models of banks and markets, technology-based innovations will lead to a significant, deeper and faster transformation in subsequent years.

b) Innovations based on technology are significant changes in the banking industry both inside and outside the country. İn customer expectations and new technological innovations to respond to changes banks began with an emphasis on the possibilities of digital experience, including on the Internet, mobile and social. As digital opportunities develop, new technologies are emerging, and customer expectations continue to evolve, banks are stepping up their efforts to transform from digitizing narrowly focused functions to broadly digitizing the

institution. These changes lead to expansion of financial participation, improvement of internal operations and transformation into the value chain of banking services.

c) **Increase financial inclusion**

d) According to the Federal Deposit Insurance Corporation (FDIC), approximately 92 million people in the US are either under-funded or non-bank, that is, they have limited access or no access to basic financial products and services, in part because of their proximity to physical branches. Technological innovations and partnerships with non-banking institutions help banks to eliminate or eliminate these obstacles. For example, regional and public banks cooperate with newcomers to provide services via mobile channels.

e) D) Improving internal operations

f) As is known, banks initially focused on adopting separate technologies for changing in narrow and specifically oriented functions (for example, implementing RPA to automate documenting processes to improve the speed and accuracy of reporting on regulatory issues). However, as technology continues to evolve and evolve, they combine many innovations to accelerate the transformation or digitization of the entire enterprise, as shown in the following graph. This includes the revision of some of the most complex and resource-intensive processes in the banking industry. For example, RPA and analytics are used to optimize anti-money laundering functions / know their clients (AML / KYC) and more effectively integrate them into a wider risk management framework.

Transformation of the value chain of a bank

Externally, non-banking organizations and other technology providers continue to enter the banking ecosystem. The growing attention of such subjects turns the value chain of the bank and accelerates the digitization of the enterprise. Banks now "internalize" or integrate non-bank entities in their business models and operating models to gain access to new customers and markets, and "externalize" non-traditional business functions to third-party service providers or utilities in order to save money and increase focus on the core Services. New technologies allow banks to revise their business models and operating models and determine which functions and opportunities should be retained internally and received from outside. Banks can take advantage of technological advances that non-banks make in several key areas

(for example, customer reporting, risk analysis as a service, blocking) by entering into a strategic partnership with these organizations. For example, some banks are cooperating with non-banking organizations to use their credit platforms to process small business lending applications faster and more efficiently.

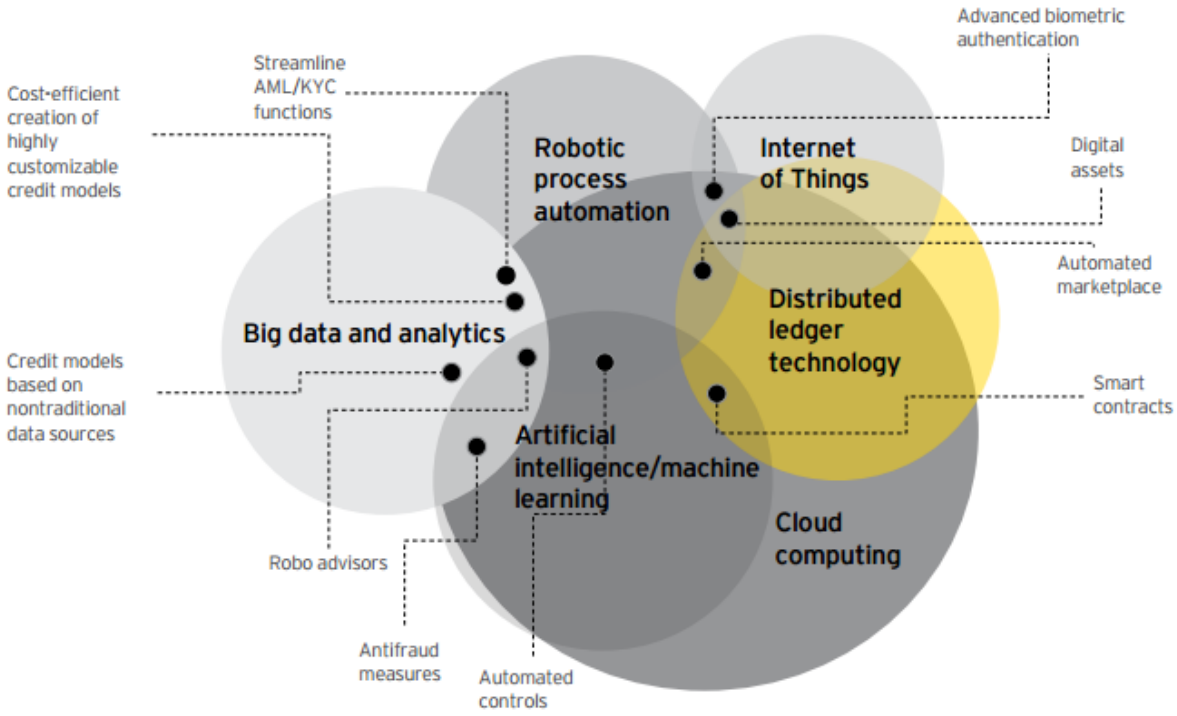

Finally, new technologies also allow centralizing some operational functions in the sectoral utilities, increasing the efficiency and sustainability of the market. This includes potential utilities for checking KYC, managing reference data and other undifferentiated services.

1.3 Value and benefits of innovation

Business models for digital bank combine problem-free user experience, in-depth analytics, scalable platforms based on cloud computing and flexible transformation methods to achieve customer focus, efficiency, resiliency and stability. Individual technologies offer various advantages to banks and customers. Nevertheless, it is convergence (i.e., interoperability and integration) of these technologies that leads to transformation across the enterprise and across the industry. Using these technologies allows banks to provide / access to value in five key areas:

•It is better to serve customers and increase access

• Provide a better understanding both in terms of risk management and in terms of customer service

• Increase flexibility and speed in the market

• Strengthen operations and control

• Transformation of institutional costs structures

Better serve customers and increase access

It is better to serve customers and increase access

Customer expectations of what looks like an "excellent" service are often shaped by their "best user experience." The optional, transparent and affordable products and services offered by leading companies of the digital age have created a new basis for the expectations of banking customers. Convenience, simplicity and interaction with customers. New technologies allow banks to minimize or even eliminate operational friction associated with interaction with the client. Banks expand access to products and services through preferred customer channels and significantly reduce / eliminate the interventions required to complete basic banking services.

ı.Enable access to basic banking services through digital channels

New technologies and the digitization of basic banking functions help to reduce dependence on access channels to banks of brick and mortar. Thanks to technologically accessible processes, such as checking the deposit through the phone, exchanging between peer-to-peer and electronic payments, banks can offer access to their products and services regardless of proximity to the bank's branch.

ıı. Expand access to additional financial products and services and create innovative new products

a) New participants of the banking ecosystem demonstrate how customers' access to banking products and services can be expanded through the use of new technologies. Examples of these new product innovations are manifested in the management of assets and assets, peer-to-peer loans and payments. The spread

of mobile access and achievements in technologies such as large data and analytics, RPA and AI, also allows banks to create new products to meet unmet customer needs. In particular, extended data sources (for example, customer-specific data sets) and new credit models that use advances in analytics expand access to credit.

b) Provide a better understanding both in terms of risk management and in terms of customer service

Over the past decade, the exponential growth of publicly available consumer and market data has stimulated the development of new technologies, including big data and analytics, natural language processing and machine learning. These technologies allow banks to analyze and analyze information about their customers and market trends by collecting and integrating information on customer interactions and IoT information (for example, chatter on social networks and other data sources that customers have "chosen"). The benefits of these innovations include: (i) increasing transparency for customers (for example, product conditions and prices) and (ii) improving institutional risk management.

I. **Increased product conditions and price transparency**
Digital business transformations aimed at improving the quality of customer service (for example, online banking) also increase the transparency of financial products and services (for example, pricing). In addition, network companies (for example, digital blogs, information collectors) also use banking websites and other sources of data on comparing financial products (for example, bankrate.com) to increase market transparency. The resulting ideas improve the decision-making process by consumers and increase the efficiency of the market.

II. **Improve risk management**
Machine learning and advanced analytics enhance risk monitoring, control and mitigation of risks in the banking industry. Banks can use enhanced internal and market data and enhanced analytics to better understand the key risk factors associated with the client and the financial transaction.In addition, enabling RPA allows banks to check transactions in real time and identify those that require additional verification. As a result of these technological innovations, banks can now detect fraud closer to real time and make it a cost-effective way with minimal disruption to the customer.

c) Increase agility and speed to market

The continued introduction of digital technology has accelerated the pace of change in the banking industry and beyond. New members of the banking ecosystem are rapidly evolving and demonstrate the feasibility of end-to-end business models with digital support. Technological innovation accelerates the transformation of banking technology and corporate architecture, allowing banks to (1) customize technologies and operations for business agility and (ii) create business models with digital support that are more sensitive to changes in customer dynamics, market and regulation.

I. **Customize technologies and operations for business agility**
Non-banking organizations; Start-ups; and large, established technology companies have demonstrated that the digital infrastructure and platforms can meet the stringent requirements of technical stability and stability (for example, systems can be constantly updated, and constant availability is maintained). Leading technology companies even commercialize their digital platforms to become public service providers. The introduction and / or integration of digital platforms within the existing infrastructure allows banks to accelerate the provision of resources, achieve scalability and maintain the development flexibility for business and IT resources to manage the business in a controlled and sustainable manner.

ii. Create business models with digital support that are more sensitive to changes in customer dynamics, market and regulation.

The transition to digital platforms allows banks to interact more closely with customers, and also to quickly develop and provide appropriate services. The digitization of end-to-end business processes also allows banks to reach a scale and become more efficient, sustainable and transparent. As a result, banks can react more quickly to market dynamics, changing customer needs and regulatory expectations. New products and services can be quickly launched, proposals quickly scaled, existing functions and capabilities are improved, and embedded and measured processes are monitored.

d) Strengthening operations and control

Digital business transformations aimed at improving the quality of customer service require reorganization, optimization and automation of business processes. These transformational efforts and the underlying technologies used to reorganize these processes can also be used to strengthen institutional operations and control. For example, digitizing manual processes with RPA support can reduce implementation costs and improve the quality and consistency of process execution. In combination with analytics, RPA also provides improved monitoring. Ultimately, integrating RPA and analytics into enterprise-level processes allows banks to achieve stronger and more efficient operations and can help in creating more robust governance structures.

- **Mitigate or prevent cases of identity theft, fraud and cyberattacks**

  Device security

  Smart network devices can identify and report attacks for companies and security vendors, which helps protect their devices and networks from penetration.

  Biometric authentication

  Identity and access management in combination with IoT allows bank managers and security personnel to receive automatic alerts about suspicious activity of customers to protect against theft and identity fraud.

  Voice recognition

  Voice recognition and analytics allow automatic identification of suspected scammers in real time, preventing repeat offenders from receiving services over the phone.

  Data analytics

  Analytics tracks the patterns of normal activity (consumer spending, internetwork data packets, etc.), and also detects and alerts users about discrepancies - reduces fraud and improves risk management.

- **Improve operational efficiency and transparency**
  Digital video surveillance platforms built into natural language processing offer cost-effective and efficient solutions for monitoring various

communication environments (e-mail, voice, text, etc.), which were previously difficult to investigate. This technology can be used to detect and prevent possible manipulation of the market by traders.The RPA can increase the sources, convert and download AML / KYC data for monitoring and reporting, improving both operational efficiency and regulatory compliance.

- **Enhancing institutional and market efficiency and resiliency**
  Banks and financial companies are currently evaluating the use of DLTs for potential efficiency gains, better risk management and / or standardization of interfirm processes. In addition to trading in financial instruments, other areas of development include the KYC creation utilities to optimize / consolidate the client verification process for the banking industry in general and supply chain management, especially with respect to trade finance. These events can further reduce costs, improve compliance and risk management, and increase the banks' ability to serve customers. In addition, the DLT's ability to provide reliable digital records protected from unauthorized access offers the prospect of enhancing operational stability for both banks and wider financial markets, as cybersecurity issues continue to grow.

e) **Transformation of institutional costs structures**
Valuation and marginal discipline continue to be key factors in the Bank's strategic decisions, especially in the context of slow economic growth. Banks can achieve these goals using technological innovations to remove costly and inefficient legacy technologies and streamline business processes. In particular, new technologies can (ı) improve the efficiency of bank costs, (ii) reduce compliance costs, and (iii) eliminate obsolete processes.

I.Improve bank cost efficiency

Digital technologies help banks move towards more modern, complex, scalable and economical platforms. RPA and analytics are used to provide significant and sustained performance improvements through automation. Today, banks evaluate and implement RPA and more advanced forms of cloud computingforremove multi-disciplinary costs, autonomously provide IT services and reduce higher operating costs.

Reducing IT costs for production through simplification, modernization and automation

• Technology reduces the cost of margin, allowing banks to simplify technological coverage, reducing production costs and increasing productivity.

• Modern sensor technologies and analytics (for example, network monitoring solutions) allow banks to better process measurements and predictability for continuous cost increases.
• Automated services, such as on-demand cloud computing, reduce IT support costs, improve IT efficiency, reduce deployment time, and maintain consistency at the enterprise level. Reducing operating costs through upgrading technologies and advanced technologies
• Now, machines can facilitate business processes (for example, automatic payments) and resolve customer and employee issues (for example, customer service). These improvements, resulting from a contextual understanding of the language, effective query matching and knowledge-based search, reduce maintenance costs.

II Reduce the cost of compliance

RPA technologies allow you to automate the intensive and repetitive reconciliation processes manually, which leads to improved quality, 24/7 performance, and cost effectiveness. Early implementation of RPA-oriented operational processes involves moving data (i.e., improving the ability of an efficient source, transforming and loading data for all forms of use from reports to analytics). Progress in analytics and artificial intelligence enhances the automation of RPA for intellectual tasks and enhances human efforts.

Reduce compliance costs and regulatory reporting

• Utilities based on cloud computing make it easy to access large amounts of data and advanced image recognition capabilities (i.e., the Analytics) to quickly identify inappropriate transactions (i.e., lead to the discovery of money laundering) and accelerate the processes of KYC.

• The logic of rules and policies can be interpreted by machines to ensure: proactive compliance control; Risk management analysis, tracking and reporting; Detection of violations; And the correction of workflow management processes.

III.Remove processes that are no longer fit for purpose in a digital era Forces such as evolving regulations, rising customer expectations,

globalization and changes in market infrastructure have driven decades of industry-wide M&A and transformation of bank business/operating models. Steps taken to accommodate these changes (e.g., expanding the role of financial market utilities) have been costly and at times hindered the adoption of industry leading practices (e.g., straight-through processing). Technological innovations have allowed banks and new entrants to augment or replace existing products, services and capabilities at a sustainably lower cost base and operating structure.

1.4 Regulatory considerations

Banks have a long and successful experience in the safe implementation of technological innovation. Nevertheless, as regulated entities, their ability to move forward in new technologies in terms of market pace can be directly influenced by the level and nature of regulatory requirements and oversight expectations. Historically, regulators have provided banks with the flexibility to develop and implement new technologies as long as appropriate control and supervision measures exist. Regulators also adapted regulatory and supervisory requirements to changing technologies and practices, as banking operations developed. The current regulatory framework sets out a wide range of requirements and expectations that relate to banking more generally, including activities that have been or will be transformed by technological innovation. In fact, when introducing technological innovations, banks face many of the same risks associated with traditional banking products and services (for example, cybersecurity, compliance, supplier / third-party management, data security, confidentiality and fraud risk). These similar risk profiles, established regulatory framework and reliable mechanisms for monitoring and managing banks allow the safe and efficient implementation of many technological innovations.

Key considerations

Policymakers and regulators continue to actively monitor developments within the banking sector, including those that are technology related, so that emerging, potential risks are appropriately addressed. Importantly, banks are

pursuing a measured approach toward the rollout of emerging technologies in order to effectively identify and appropriately manage any new or different risks and to comply with associated regulatory requirements and supervisory expectations. Banks are also coordinated on an industry basis to develop effective protocols and controls, not only to protect their respective institutions, but also to address any possible systemic consequences.But, gaps and / or inconsistencies within the regulatory framework, both domestically and internationally or in both cases, can increase uncertainty for banks during the innovation process. In order to solve these problems, policymakers, regulators and industry must expand their activities with each other - both internally and internationally - as this will enable policymakers and regulators to stay abreast of rapidly evolving technologies and to promote more innovative innovations in a timely, safe and effective way.Moreover, policymakers and regulators should also coordinate their activities internally and internationally to provide the industry with a clear and consistent message about the regulatory requirements and expectations for the supervision of technological innovation. This is particularly important given the global reach of many banks, the market infrastructure and technology providers, and the prevalence of overlapping regulatory bodies with respect to these entities within individual jurisdictions. To date, banks have safely implemented many useful technologies without adverse consequences for institutions or a wider financial system. Nevertheless, the introduction of technological innovations, especially new technologies, will always have some element of risk, given the heuristic nature of innovation and new activities and services. In the future, appropriate levels of capital, liquidity and operational sustainability, as well as effective management of technological innovation and reliable internal controls, should help limit any potential negative consequences arising from the development of new technologies. A supervisory review of these safeguards will enable banks to safely learn new technologies without requiring specific licensing requirements for them.

1.5 Mobile Banking

M-banking is next version of Internet banking. M-banking makes use of a mobile terminal to perform banking transactions. It combines currency electronation and mobility to offer a new kind of banking service and allows

people to perform many different kinds of banking service at anytime, anywhere. In adopting M-banking there are some advantages as follows: No restrictions in location: The user can perform banking activities at any time in any place. High penetration: The popular utilization of mobile phones provides a sufficient assurance of the growth and utilization of M-banking. Personalization: Each mobile phone is dedicated to a specified user. Therefore, it increases the effectiveness of user authentication. Existing system M-banking verification scheme with OTP(one time password) and a single personal biometric trait(image/ video) provides better reliability as well as security. In this scheme, the user (client) can perform any query/browse/money transaction type of operation, simply by registering on the web page with their respective user ID & password. The server then verifies client's id & for correct id, server sends an OTP on user's request for the transaction. When OTP is checked by the server, it asks the user to upload its biometrics. Finally, the user gets access to the beginning of a transaction with money if its corresponding loaded biometrics coincides with the registered in the database. Using multimodal biometrics for M- banking - System can retain a high threshold recognition setting and system administrator can decide the level of security that is needed. Hence by using combination of multiple sources of information, systems improve matching performance, Increase population coverage. The One-Time Password (OTP) system is a Two-Factor Authentication system in which the password constantly alternates whenever used. Due to which the risk of an unauthorized intruder gaining access to the account reduces to great extent. In OTP Password Generation, it uses a hash function for the generation of password. The one-time password system works by starting with an initial seed, then generating passwords as many times as necessary. The table mentioned below gives a comparison of various M-banking schemes along with the factors & functions they provide:

Functions	M-Banking Scheme		
	Traditional OTP verification scheme	OTP and biometric(single biometric)verification scheme	Proposed OTP and multimodal biometrics verification scheme
OTP	Randomly generated	Randomly generated	Randomly generated
Webpage verification	Randomly generated	Randomly generated	Randomly generated
Password transfer via internet	Plain text	Ciphertext	Ciphertext
Biometric verification	No	Yes	Yes
Recognition performance	Poor	Moderate	Better

Table1.Comparison of various M–Banking schemes along with the factors&functions

Indexing is the process of assigning a numerical value to a database entry, in order to facilitate its rapid retrieval. For example, while indexing a fingerprint database it helps in reducing the search space and improves the response time of an identification system. In biometric identification systems, the identification of input data is determined by comparing it with each record of the database. This process increases the response time of the system and, possibly, the speed of identification.The method, which narrows the list of potential identities, will allow to compare the input data with a smaller number of identifiers. We describe the method of indexing large-scale multimodal biometric databases which is based on the index code generation for each registered identifier.The index code is created by calculating the matches between the biometric input image over a fixed set of reference images. Depending on the similarity between the index image code of the input probe and the identifiers in the database, images are extracted.

Proposed work

The project main idea is based on Multi-factor authentication. The project has two main parts; registration and transaction. The page for sign up has the

details like; name, address, phone number and insert face, iris and finger images. The data is stored. The biometric data is multimodal. The fused matrix can be used for comparison. In translation, user will enter the ID, an OTP is generated. He will enter the OTP. Once OTP is correct, then the biometric identification is required. In this user should select the same images for finger, iris and face, which were inserted during registration we will choose the images from the folder.The biometric data is compared with registered data. If inserted datamatches, then the user will be allowed for next processing. The various algorithms for image comparisons are described below. For finger comparison, we are using morphological method, for face comparison, we are using the PCA method and for iris comparison, we are using DCT (discrete cosine transforms) based method. The steps of the project can be described as below.

For finger comparison, we are using morphological method. The flow of the project can be shown as below.

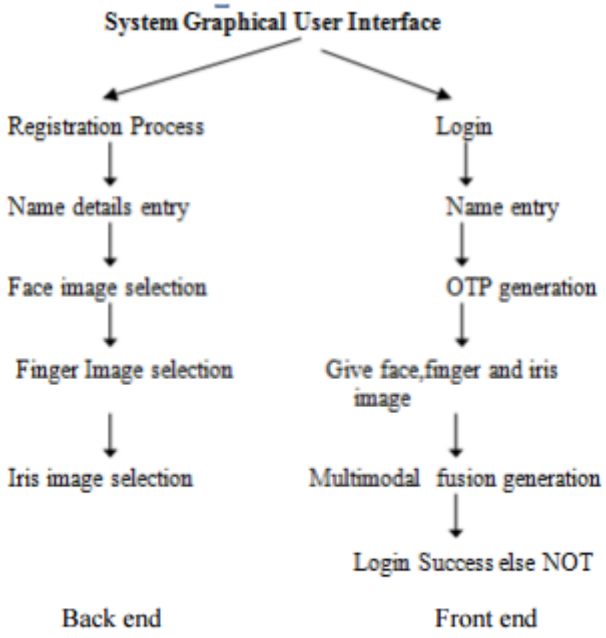

Fig. 1 Proposed system design flow.

Chapter 2 Biometrics

2.1 Introduction to Biometrics

With the growing importance of security, the need for an automated personal biometric authentication system is increasing. Because traditional authentication systems based on cards or passwords can be broken by losing or stealing cards and forgetting passwords. Thus, there is a need to identify systems for identifying people that are independent of what person has a card or not, or what a person remembers. Biometrics can be divided into two main classes: physiological and behavioral. The physiological class is associated with the shape of the body, including a fingerprint, face recognition, DNA, palm print, hand geometry and iris recognition. The behavioral class is associated with human behavior and includes a gaining rhythm, gait and voice. Recently, the recognition of the iris becomes one of the most important biometrics used in recognition, when the image can be made at a distance of less than two meters. This value is due to its high reliability for personal authentication.Human iris has a great mathematical advantage that its variability in different people is very high, because the iris has a high degree of randomness. In addition, iris is very stable over time. Since the concept of automatic recognition of the iris was proposed in 1987, many researchers worked in this area and offered many powerful algorithms. These algorithms were based on a variety of iris texture and can be divided into many approaches, phase methods, a representation with zero intersection, texture analysis and intensity variations. The most appropriate algorithms and widely used in current real applications are the algorithms developed by Daugman.

There are many commercial iris capture systems capture images of the iris using near

recognition systems.

2.2 Biometrics

Biometrics is a technology consist of methods for identify, measure, and analyze an individual’s behavioral and physical characteristics. Another definition defines biometrics as the science and technology of measuring and analyzing biological data. In information technology, biometrics refers to technologies that measure and analyze human body characteristics, such as fingerprints, eye retinas and irises, voice

patterns, facial patterns and hand measurements, for recognition purposes. Biometrics can be divided into two main classes

 Physiological: are related to the form(shape) of the body. Examples include, but are not limited to manual geometry, face recognition, DNA, palm print, fingerprint iris recognition, which has broadly replaced the scent and retina.

 Behavioral: are related to the behavior of a person. Examples include, but are not limited to gait, voice and typing rhythm. The voice can sometimes be considered as a physiological feature, because each person has another vocal tract, but voice recognition is determined through the person speaking, so it is usually classified as behavioral.

One can understand whether a human trait can be used for biometrics in the following parameters:

 Universality – each person should have the characteristic.

 Uniqueness – each person has unique traits that differ individuals one from another and uniqueness is how well the biometric separates individuals one from another.

 Constancy - measures the stability of biometrics to aging and another variance over time.

 Collectability – ease of collecting for measurement.

 Performance - accuracy, speed and reliability of the technology used.

 Acceptability is the degree of adoption of technology.

 Circumvention – ease of use of a substitute.

The first time a person uses a biometric system, this is called enrollment. Personal biometric information is retained during registration. For the following purposes, biometric information is found and compared with information entered and stored at the time of registration.

Figure 2.1 shows the basic block diagram of a biometric system.The first is the interface between the real world and the system; He must receive all the necessary data. In most cases, it is an imaging system, but it can vary according to the desired

functions.In the second part of the scheme, all the necessary initial processing is realized: it must remove artifacts from the sensor, improve the input (for example, remove background noise), use some kind of normalization, etc. And the last step, which is an important step to extract the correct functions by an optimal way.To create a template, use a vector of numbers or an image with special properties. A template is a synthesis of suitable characteristics extracted from a source. Some elements of the biometric measurement that are not used in the comparison algorithm are removed from the template to reduce the file size and protect the identity of the person. If registration is performed, the template is simply stored somewhere (on the card or in the database or in both cases). If the authentication step is performed, the obtained template is compared with other existing templates, estimating the distance between them using any algorithm (for example, the Hamming distance).

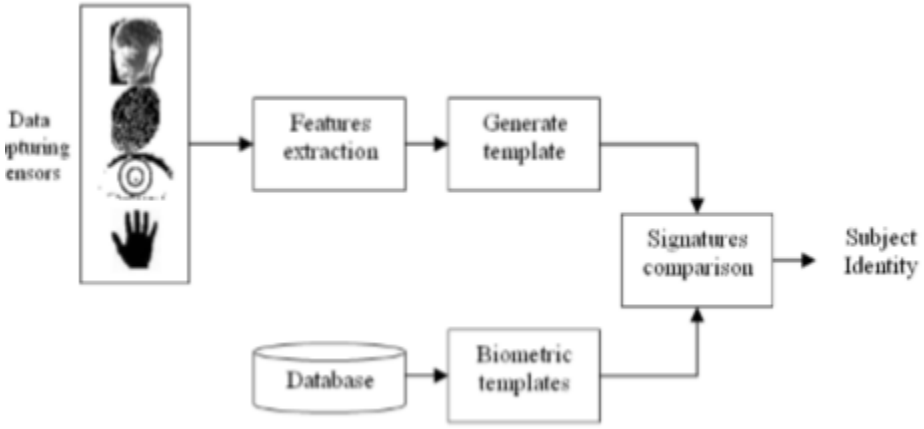

Figure 2.1: The basic block scheme of the biometric system.

If the distance between the templates is less than the specified threshold, it is possible that two compared templates will be mapped and vice versa. The most common biometric data that is currently used for security purposes are:

DNA

Deoxyribonucleic acid (DNA) is unique for each person, represented by a one-dimensional code. The only identical twins are exceptions, which can cause a serious problem with regard to security and forensic applications.It is believed that this method has some drawback, since easy contamination and sensitivity, the

impossibility of real-time recognition and serious problems with confidentiality, since DNA can detect susceptibility to certain diseases.

Face

Facial images are the most common biometric characteristic used by humans to perform personal recognition because this is a non-intrusive and suitable trait to perform covert recognition. There are three types of methods for distinguishing features: general methods based on lines, edges, and curves; Based on patterns that are used to detect facial features, such as eyes and structural matching methods that take into account the geometric restriction of functions.Despite the fact that the efficiency of commercially available systems is reasonable, there are still significant opportunities for improvement, since the false reception rate is about 1%, and the false-rejection rate is about 1%. These systems face severe difficulties when faces are captured at different angles and uncontrolled environmental lighting.

Fingerprint

Used for many centuries, creating an ink seal of its patterns or using a reader, access to the details of fingerprints and furrows associated with certain points of detail can determine its uniqueness. Although it is mature and easy to use, it also requires user interaction and is vulnerable to noise.

Gait

Despite the fact that it was originally performed using physical devices worn on the subjects' feet, the gait biometrics based on sight recently received a lot of attention, and the first known attempt to recognize was done by Niyogi and Adelson in the early 1990s.The human gait is a periodic movement with each gait cycle, encompassing two steps: the left foot forward and the right foot forward. Each step covers a double support stand on the foot together when the legs swing from each other and return to the dual support position. Reported weather vulnerabilities to changes in conditions of transportation, walking speed or on the surface of walking. Due to these biometric systems based on gait represent high values of false failures. In addition, it is considered one of the most expensive methods, because the video sequence is used to collect the required data.

Iris

Iris is a complex pattern that contains many characteristic features, such as furrows, arching ligaments, ridges, rings, crypts, freckles, crown and zigzag collage. Each iris is unique for each person, and even the irises of identical twins are different. Moreover, the iris is shown easier than the retina; It is very difficult to surgically manipulate information about the texture of the iris, and you can find artificial irises. Although the original iris-based identification systems were expensive and required significant user participation, efforts are continuing to create more economical and user-friendly versions. To get a good image of the iris, the iris is usually illuminated by near-infrared identification systems, as seen in most cameras, but not detected by humans. The available results of both the speed and the accuracy of the diaphragm identification are very stimulating and indicate the possibility of large-scale recognition using diaphragm information. Although this estimate depends on a specific goal, because of this and with the characteristics described above, it is considered that the rainbow is one of the best biometric features.

Keystroke

Behavioral biometrics "Dynamics of keystrokes", using the manner and rhythm in which a person types characters on the keyboard or keyboard. First, the user's keystrokes are measured to create a unique biometric template for the user input template for future identification. The raw measurements available on each keypad can be recorded to determine the flight time (the time between the up and down keys) and the waiting time (key press time). Then, the recorded keystroke data is processed to determine the primary template for future comparison. In addition, vibration information can be used to create a template for future use in identification and recognition tasks. Unlike other features, information about keystrokes can be continuously analyzed by the recognition system, reducing the probability of active forged measures. Moreover, since users have a habit of authenticating themselves through user names and passwords, most biometric keystrokes are well perceived by users and are completely transparent. Among potential weaknesses, confidentiality considerations should be taken into account, since the method of subjective strokes can be used to derive information about performance and its potential profitability.

2.3 Performance of Biometrics

The biometric system can work under two conditions, verification and identification. The following two subsections describe these modes and how we can evaluate their performance.

2.3.1 Verification

Checking. In this state, each captured biometry is compared to each other with a saved pattern to check whether the person is the one who is said to be. As a result, if two samples match enough, the identity card is checked, and if the two samples do not match well enough, the request is rejected. A smart card, number or username can be added to the verification.

There are four possible outcomes in a verification decision context normally called:

1. False Accept Rate (FAR) or False Positive (FP) or False Match Rate (FMR):

 Occurs when the system accepts an identity claim, but the claim is not true.

 The proportion of forgers attempts whose Hamming Distance (HD) is below a given threshold.

2. Correct Accept (CAR) or True Accept (TA) or True Positive (TP):

 Occurs when the system accepts, or verifies an identity claim, and the claim is true.

3. False Reject (FRR) or False Negative (FN) or False Non Match Rate (FNMR):

 Occurs when the system rejects an identity claim, but the claim is true.

 The proportion of original or authentic attempts whose Hamming Distance(HD) exceeds a given threshold.

4. Correct Reject (CRR) or True Reject (TR) or True Negative (TN):

 Occurs when the system rejects an identity claim and the claim is false.

In the verification scenario, biometric characteristics are often summed up in the receiver performance curve (ROC). The ROC curve shows the false reception speed on the X axis and the Y-axis test speed, or alternatively the false-reception value on the X-axis and the false-y-axis coefficient. A single number called the Equal Error

Rate (EER) is often specified from the ROC curve and indicates that the FNMR and FMR are the closest peers. Equal error rates allow you to evaluate FNMR and FMR at the same operating point.

2.3.2 Identification

Identification is one of many comparisons of a captured biometric with a biometric database or gallery (the Gallery is a collection of registered samples) in an attempt to identify an unknown person. If the comparison of the biometric sample with the template stored in the database falls into the specified threshold, then the identification of the person is completed successfully.

Like verification mode, there are four possible results normally called like verification in identification decision context: -

1. False Accept Rate (FAR) or False Positive (FP) or False Match Rate (FMR):

 Occurs if the system says that an unknown sample matches a particular person in the gallery but the match is not true.

 The rate at which the matching algorithm incorrectly determines whether the biometric forger pattern matches the registered template.

 The proportion of forger attempts whose HD is below a given threshold.

2. Correct Accept (CA) or True Accept (TA) or True Positive (TP):

 Occurs if the system says that an unknown sample matches a particular person in the gallery and the match is correct.

3. False Reject (FR) or False Negative (FN) or False Non Match Rate (FNMR):

 Occurs if the system says that the sample does not match any of the entries in the gallery, but actually the sample does belong to someone in the gallery.

 The proportion of original or authenticated attempts whose HD exceeds the specified threshold.

 The degree at which a matching algorithm incorrectly fails to determine that an original sample matches an enrolled sample.

4. True Reject (TR) or True Negative (TN) or Correct Reject (CR):

 Occurs if the system says that the sample does not match any of the entries in the gallery, and actually the sample is not in the gallery.

Performance is often summarized in the Cumulative Match Characteristic (CMC) curve in the identification script. The CMC curve displays the cumulative rank, considered as the correct X-axis match, and the percentage of probes correctly recognized along the Y axis.

Of course, the first and third results in the two states of verification and identification are incorrect, while the second and fourth results are sought. By managing the decision criteria, the relative probabilities of these four outcomes can be adjusted in such a way that they reflect the costs and benefits associated with them. The values of these values can vary greatly in different applications. In the context of the customer, the cost of the FRR error may exceed the cost of the FAR error, while the opposite may be true in a military context.

The idea of a solution landscape is illustrated in Figure 2.2. Two distributions are imperfectly separated two states of the world. Abscissa is any metric of similarity or dissimilarity; In this case, this is the Hamming distance, which is the fraction of bits that is different between the two binary strings. The decision as to whether they are instances of the same template or completely different templates is done by imposing a certain decision criterion for the similarity indicated by the dashed line. The similarity in comparison with some Hamming distance (0.4 in this case) is considered sufficient to treat patterns as one and the same, but outside this point, the models are declared as different.

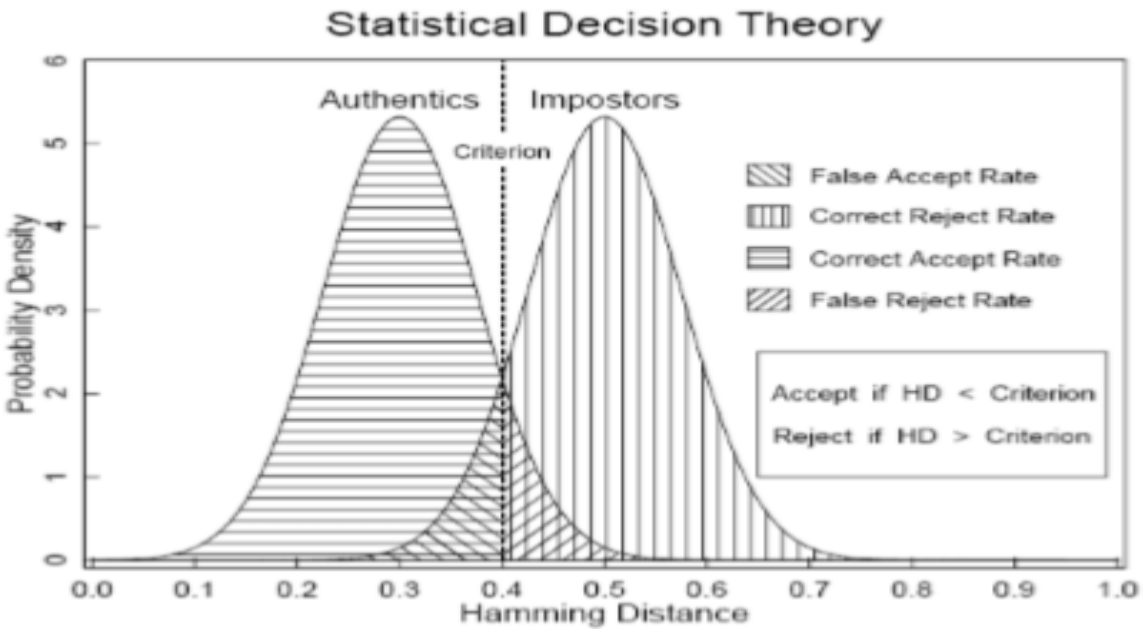

Figure 2.2:Decision landscape: general formalism for biometric decision making

2.4 Iris Anatomy

The iris is a thin circular eye structure consisting of a pigmented fibro-vascular tissue known as the stroma. Stroma connects a set of stretch muscles and sphincter muscles to open it. It is divided into two main areas: the pupil is the inner region, and the ciliary zone (Iris) is the rest of the iris.The pupillary zone is the inner part of the iris, the edges of which form the border of the pupil. The ciliary zone is the outer part of the iris, which extends to its beginning in the ciliary body. The area that separates the pupillary zone from the ciliary zone is designated as a collarette. The sphincter and the muscles of the dilator overlap in this area. An example of an image from the UBIRIS iris database and the areas of each part of the iris is shown in Figure 2.3.

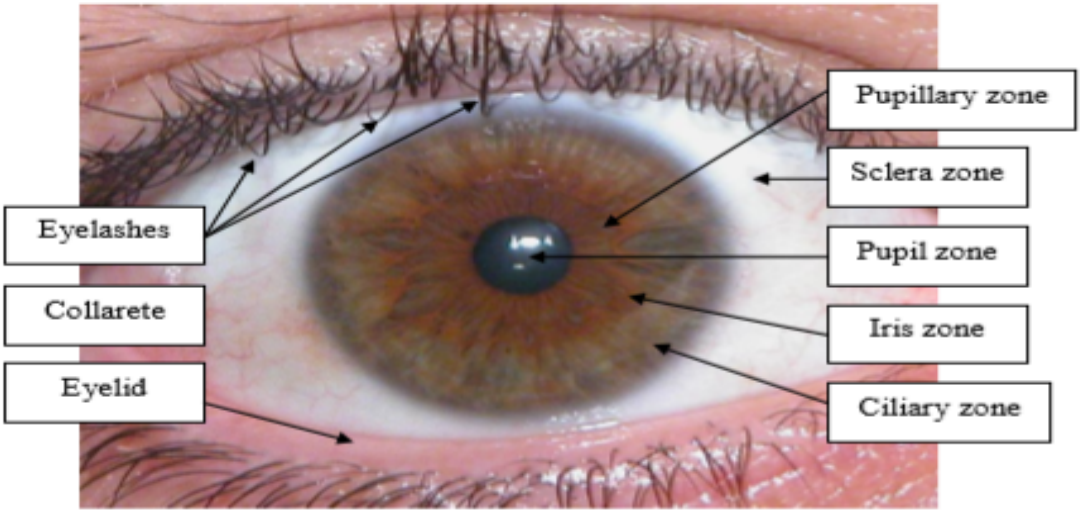

Figure 2.3: Morphology of the human iris (UBIRIS Database).

Iris begins to form during the third month of pregnancy, and the structure is fully formed for the eighth month, although the pigmentation continues in the first year after birth. The visible features of the iris appear in the trabeculae, which are the retina of connective tissues with arching connections, crypts, tendinous furrows, a crown and pupil frill, color and freckles. Although the front layer creates the predominant iris texture visible with visible light covering the trabecular mesh, additional distinctive information can be specified by the arrangement of all these sources of radial and angular variation. Together, as Daugman mentioned, they provide an outstanding and unique signal.

It is believed that the texture and detail of the iris have a high random morphogenesis and do not have genetic penetration in its expression. Since the appearance of each iris depends on the initial conditions in the embryonic mesoderm from which it develops, a phenotypic picture of two irises with the same genetic genotype (for example, identical twins or both eyes of the subject) gives out small things. Past studies on the texture of the iris concluded that the interdisciplinary variability of its structure covers about 250 degrees of freedom and has an entropy of about 3.2 bits per square millimeter. The chaotic appearance of the iris and these biological characteristics have turned it into one of the most suitable traits for biometric

purposes. Iris is usually considered one of the most promising biometric features and is a topic for developing and proposing many algorithms for biometric recognition.

Chapter 3 Literature Review

In this section, we describe the most common used iris recognition methods. Then we review the common segmentation methods used in iris recognition. Finally, describe the pupil dilation and analyzing iris code.

3.1 Methods of iris recognition

Although there are many proposed iris recognition systems, they all roughly share the following main stages: iris segmentation, iris normalization, feature extraction and feature comparison, as shown in Figure 3.1. In this chapter, we explain in detail the stages of the most common methods in the iris recognition system.

3.1.1 Daugman’s Method

The concept of iris recognition was first proposed by Dr. Frank Birch in 1939. In 1990, it was first realized when Dr. John Daugman created algorithms for her. These algorithms apply image recognition methods and some mathematical calculations for the recognition of the iris. In 2004, Daugman's new article stated that imaging should use infrared lighting to control lighting.

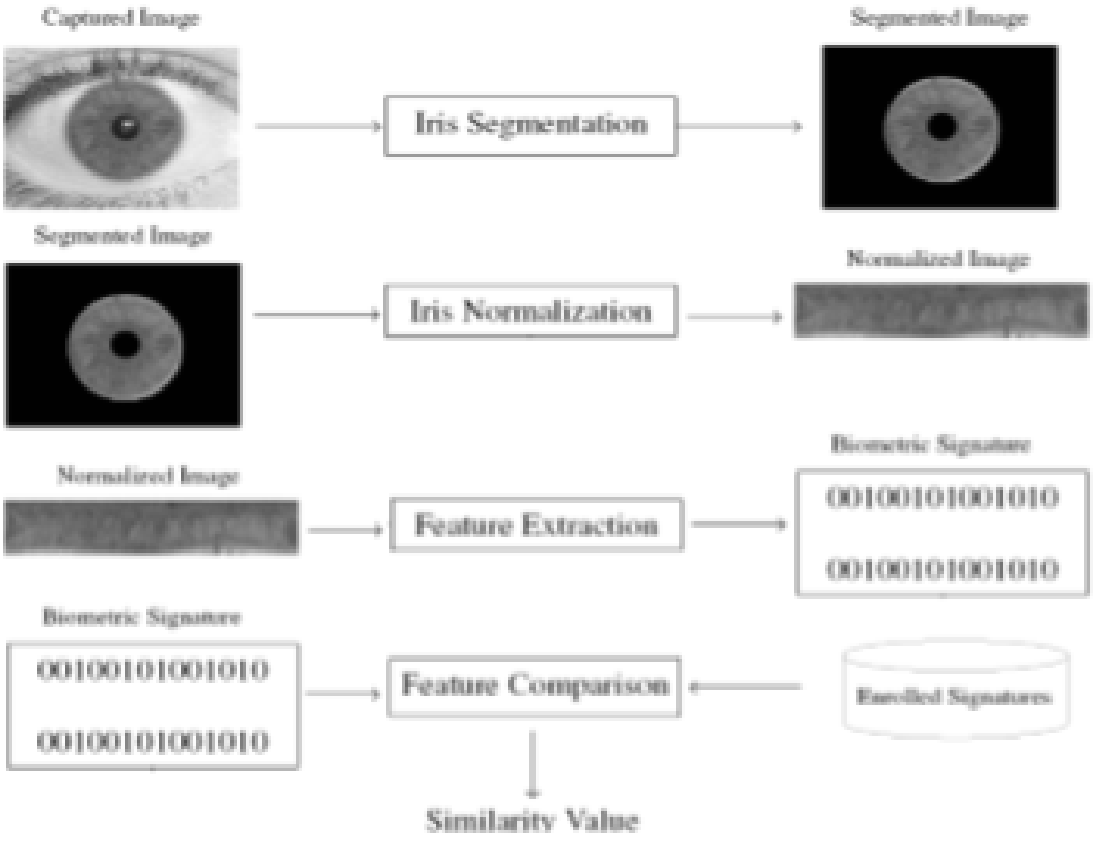

Figure 3.1: The main stages of iris recognition systems.

Lighting in the near infrared range also helps to clarify the detailed structure of dark (heavily pigmented) irises, and the iris is localized from the image in the next step. Daugman approximated the pupil and the iris of the eye as circles. Thus, he proposed an integral-differential operator for the search and contours of the iris and pupil. Since all the images of the diaphragm are of different sizes (for example, the distance from the camera affects the size of the iris in the image, the angle of the image capture, and the variation in illumination), Daugman proposed a rubber sheet model for normalizing the diaphragm after segmentation. The iris is processed from the raw Cartesian coordinates (x, y) into a dimensionless polar coordinate system. This coordinate system consists of pairs of real coordinates (r, θ), where r is in the unit interval, and θ is the angle of an inch. It is used to ensure that all irises are of the same size and also simplify the following treatment.

Dagman applied the Gabor filter, which is a two-dimensional texture filter that refers to the image of the iris for holding out the signs from the iris after normalization and extracts a part of the texture called the iris code.

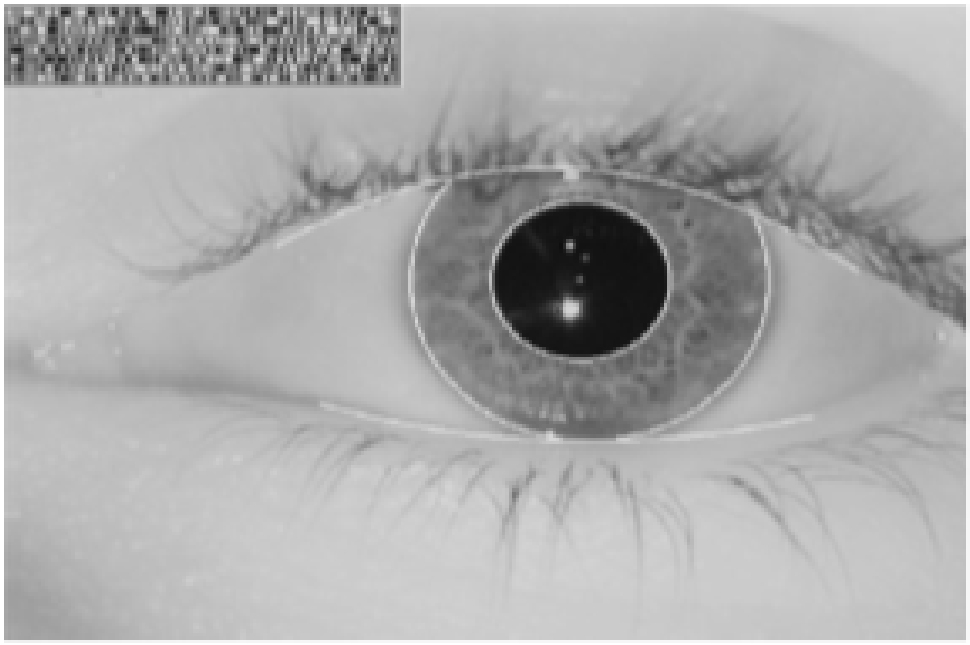

Figure 3.2: Example of an iris with its iris code

The iris code is a binary representation of iris. It is a set of bits, each bit of which indicates whether a given bandpass texture filter (Gabor filter in Daugman algorithm) applied at a given point on the iris image has a negative or nonnegative result. In figure 3.2 shows example of iris code. Daugman used Hamming distance to compare two iris templates as the similarity measure for two iris signatures.

With N bits, each given two binary sets, A and B: where A = {a1, ..., aN} and B = {b1, ..., bN}, the Hamming distance is:

$$HD(A,B) = \frac{1}{N} * \sum_{i=1}^{N} (a_i \otimes b_i)$$

where $\otimes$ is the logical XOR operation. Thus, if two signatures are completely equal the value of the Hamming distance will be zero, and if signatures are completely different, the value of the Hamming distance will be one.

3.1.2 Wildes' Method

Wildes used various methods from Daugman's methods to describe the biometric system of the iris. Wildes used a gradient-based binary structure of the edge map, and then a circular Hough transformation to achieve iris segmentation. In the segmentation of the diaphragm, this method became the most common method, later many researchers suggested that the new algorithms depended on this method.

Wildes used a Laplacian of Gaussian filter at multiple scales to generate a template and compute the normalized correlation as a similarity measure after normalizing the segmented iris.In this method, he used the technique of registration images for compensate rotation and scaling then an isotropic band-pass decomposition is proposed, derived from application of Laplacian of Gaussian filters to the image data. In the comparison phase a procedure is used which based on the normalized ratio between both iris signatures.

Although the Daugman system is simpler than the Wilde system, the Wildes system has a less affected light source, designed to eliminate mirror reflections. It is expected that the approach of Wildes will be more resistant to noise disturbances, it will reduce the use of available data due to the binary abstraction of the edge and, therefore, may be less sensitive to certain details. In addition, the approach of Wildes involved the detection and localization of the eyelids.

3.1.3 Key Local Variations Method

Tieniu Tan, Li Ma, Dexin Zhang and Yunhong Wang described key local variations and proposed a new algorithm for recognizing the iris. In this algorithm, the basic idea is that local points of sharp change, indicating the appearance or disappearance of an important image structure, are used to represent the characteristics of the iris. First, the background is removed in the iris image, localizing the iris, approximately defining the area of the iris in the original image. And after determining the area of the iris, use the Hough transform and the edge definition to accurately calculate the parameters of the irises in a certain area. To achieve immutability during translation and scaling, the annular iris region is normalized to a rectangular block of fixed size using an algorithm. Then, the image and lighting are improved to handle the uneven brightness and low contrast caused by the light position of the sources. In Fig. 3.3 shows the phases of segmentation and normalization.

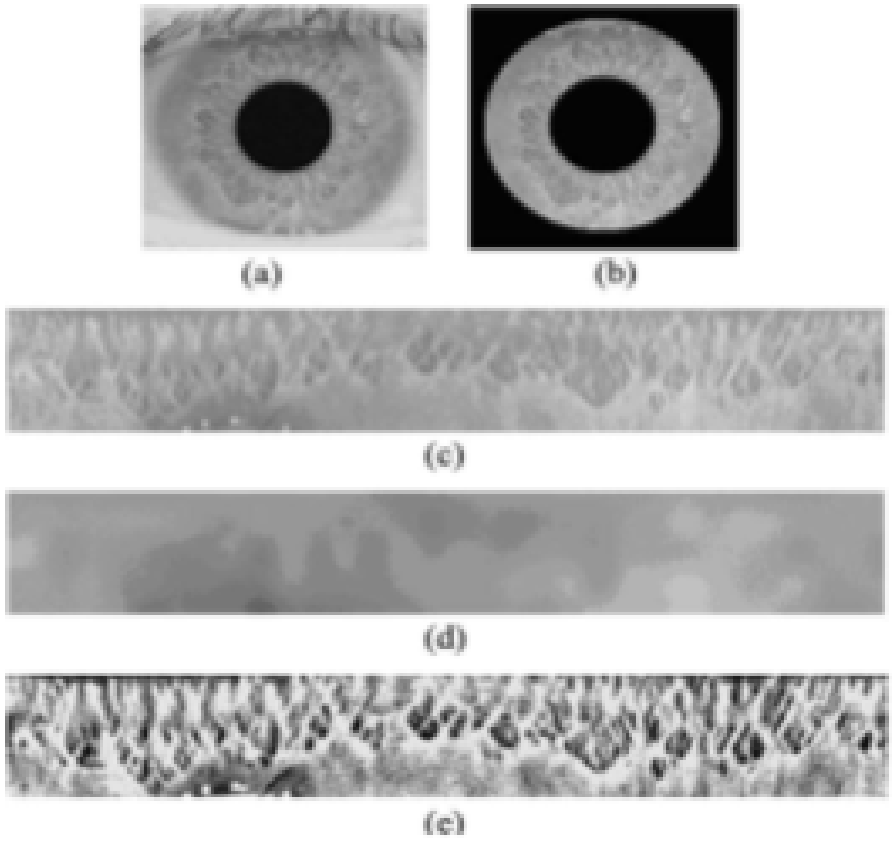

Figure 3.3: Iris image preprocessing: (a) original image. (b) localized image. (c) normalized image; (d) The estimated local mean intensity. (e) enhanced image

They create a set of signals of intensity 1-D in the stage of extraction of signs. It contains the main variations in the intensity of the original iris for subsequent extraction. They note the position of local points of sharp change, using the wavelet analysis in each intensity signal as a function. The correspondence of a pair of sequences of positions is also very troublesome. Thus, to solve this problem, they accept a fast matching scheme based on the exclusive OR operation.

3.2 Segmentation Methods

Many researchers have made a great contribution to the method of segmentation. They used various methods and methods to improve the performance of their algorithms. Previous algorithms can be divided into two classifications: according to

the region of the beginning of the segmentation and according to the operators or methods used to describe the figures in all eyes.

Classification by region began.

Researchers are divided into three categories depending on where they begin segmentation. Researchers belonging to the first category, break away from the pupil. Because this is the darkest area of the image. Proceeding from this, the pupillary border of the iris is fixed, and the pupil is localized, then the diaphragm is determined in various ways. Finally, they detect noise and isolate from the area of the iris.

Studies of the second category begin with sclera. Since the part of the sclera is less saturated (white) than other parts of the images, especially for images exposed to noise or images containing heavily pigmented (dark) irises, or. After determining the scleral region, the iris is detected using any methods. Finally, they detect the pupil and noise and isolate from the area of the iris.

Researchers belonging to the first category, directly search for the area of the diaphragm, apply clustering algorithms, or use boundary operators to extract texture features of the iris.

Classification of the operations used to describe figures in the eyes.

There are two main opinions about the localization of the iris area in accordance with the methods used. The first method uses the edge detection type or one of its derivatives to determine the shape of the pupil and iris, sometimes a final phase is used to correct the shape of the pupil or iris.

This type uses various methods to detect the edges of the iris, such as the Daugman Integro-differential operator or the Camus and Wilde method, and use the same operator or another to remove the pupil area.

In the following subsections we explain the most famous and strong segmentation methods because of their relevance in the literature.

3.2.1 The Daugman Method

The method of Daugman is most commonly used in the literature on iris segmentation. This method is licensed for Iridium Technologies1, which turned it

into the basis of 99.5% of commercial iris recognition systems. This was proposed in 1993. This was the first method, effectively implemented in the working biometric system. Both pupil and iris are taken with a circular shape and apply the following operator

$$max(r,x0,y0) = |\mathrm{G}\sigma(\mathrm{r}) * \frac{\delta}{\delta r}\oint \frac{I(x,y)}{2\pi r} ds$$

I(X, Y): the original iris image. r0,X0, Y0 are the radius and center of brute circle (for each of iris and pupil). $\mathrm{G}\sigma(\mathrm{r})$ isGaussian function. Δr is the range of radius for searching. $\mathrm{G}\sigma(\mathrm{r})$is a smoothing function, the image is then scanned for a circle after smoothing, which has the maximum gradient change, which indicates the edge. This operator works very effectively on images with sufficient separation between the values of the intensity of the iris, pupil and sclera. But, if the images do not have a sufficient degree of separation, especially between the sclera and the areas of the iris, then it often fails. If there are noise types in the image of the eye, such as reflections, then this algorithm can also fail. Thus, it works perfectly only on images that were selected on a near infrared camera and under ideal shooting conditions.

3.2.2 Camus and Wildes' Method

Camus and Wildes created an algorithm for searching the iris of an object in a large image. This algorithm, used both for pupil boundaries and for iris, is the metric of the fitness component for suitable boundary parameters considered with respect to the given C for the polar coordinate system.

$$C = \sum_{\theta=1}^{n}\left((n-1)_{||}\mathrm{g}\theta,\mathrm{r}|| - \sum_{\varphi=\theta+1}^{\infty}(||g_{\theta,r} - g_{\varphi,r||}) - \frac{I_{\theta,r}}{n}\right)$$

where n is the total number of directions and $I_{\theta,r}$ and $g_{\theta,r}$ are, respectively, the image intensity and derivatives with respect to the radius in the polar coordinate system.

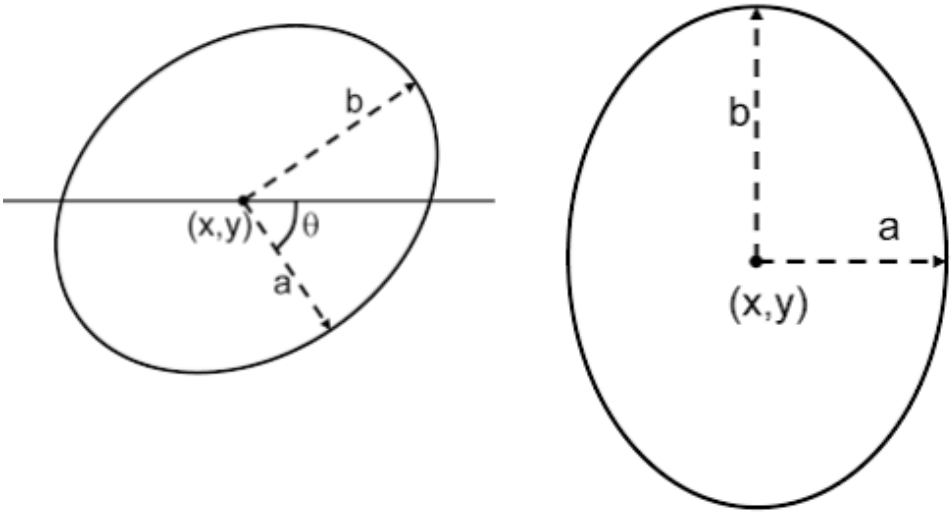

Figure 3.3.1 Curve Fitting

This methodology is very exact on images where the iris and pupil regions' intensities are clearly separated from the sclera ones and on images that contain no noise factors or reflections. When dealing with noisy data, the algorithm's precision corrupts significantly.

3.2.3 Wildes' Method

This is an automatic segmentation method, based on Hough's circular transformation, developed by Wildes. In this algorithm, the outline setting is performed in two stages. In the first step, information about the intensity of the image is converted into a binary edge map. And the second step, the edge points suggest illustrating concrete values of the contour parameters. The offering procedure is performed via Hough transforms. The parameter with largest number of offers (edge points) is a possible choice to represent the contour of interest. Recently the second step is called circular Hough transform. There are many problems with the Hough transform method. It requires initial values to be chosen for edge detection and the Hough transform is computationally intensive due to its Brute-force approach which may not be compatible for real time applications.

3.2.4 Proenca Method

Proenca used an algorithm to segment degraded images achieved at the visible wavelength. It consists of two parts: in first part iris regions without noise are detected and in second part the iris shape is parameterized. The initial stage is further divided into two processes: in first process the irisis detected and in second process the sclera is detected. The basic concept is that the sclera is the most easily attractive area in non-ideal images. Next, he operated the mandatory adjacency of the iris and the sclera to detect iris regions without noise. He noted that the whole process consists of three tasks, which are usually divided in the literature: detection of the iris, segmentation and detection of noisy (occluded) areas.

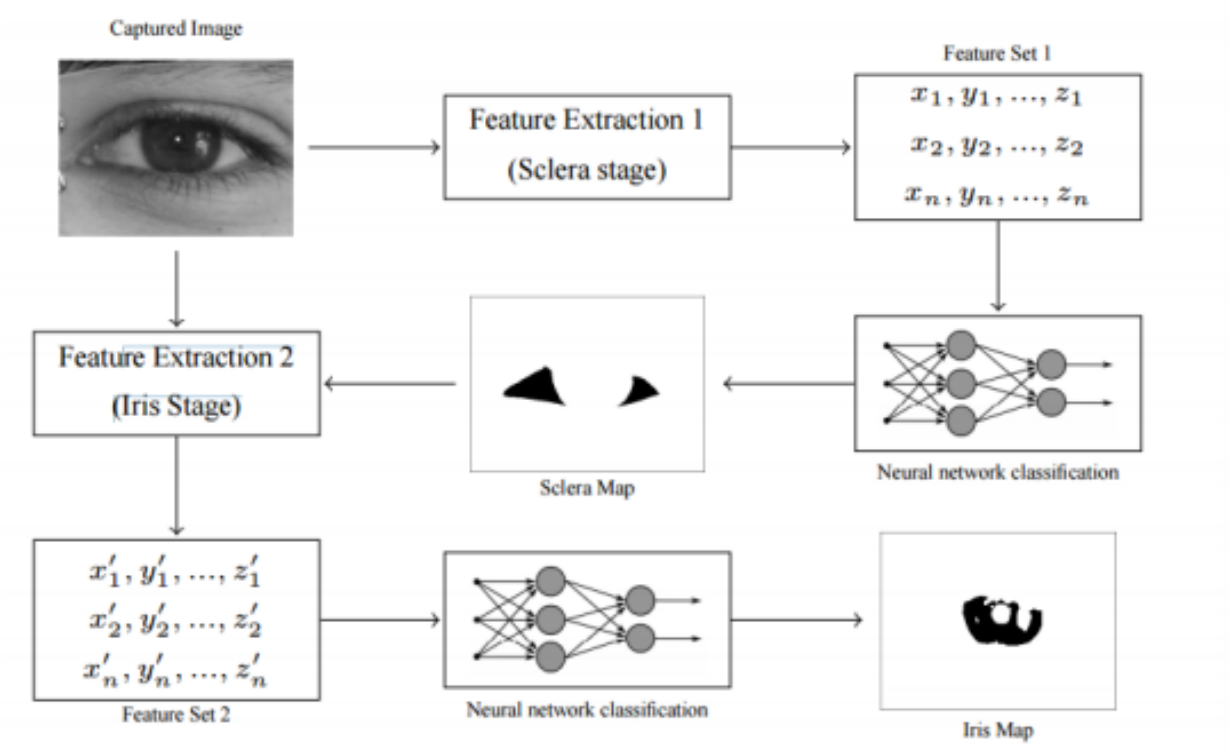

Figure 3.4: Block scheme of Proenca segmentation method

The second part of the algorithm consists in parametrizing the detected area of the iris. In the end, a small inaccuracy of the classification near the boundaries of the iris is processed using the method of limited polynomial selection, which is fast and able to regulate figures with an arbitrary degree of freedom, which naturally compensates for this inaccuracy. In figure 3.4 shown a scheme diagram of Proenca segmentation method. Although the Proenca method is very accurate with noisy images that are

perceived at the visible wavelength, it depends on the sclera from determining the area of the iris, if a sclera covered with dark colors caused by eye diseases or a poorly displayed environment, then the algorithm may fail.

3.3 Previous Research in Pupil Dilation

As mentioned earlier, there are few researchers who discussed the problem of pupil dilatation and its effect on the iris recognition system. In this part, we are considering some of these studies.

Figure 2.4: Block diagram of Proenca segmentation method.

Daugman's Rubber Sheet Model

Daugman solves the problem of dilation of the pupil by re-mapping each point inside the iris region into a pair of polar coordinates (r, θ), where r is in the interval [0,1], and θ is the angle [0,2π]. In the model of a rubber sheet, dilation and dimensional discrepancies of the pupil are taken into account to obtain a normalized representation with constant dimensions. Thus, the iris region is modeled as a flexible rubber sheet fixed at the border of the iris with the center of the pupil as a reference point. Although the model of a uniform rubber sheet explains the image distance, pupil dilation and displacement of nonconcentric pupils, it does not compensate for the nonlinear dilation of the pupil. Daugman suggests that when the pupil expands, it is an iris in a linear fashion, but this is not accurate. Many irises are non-linear, when their pupil expands, which will affect the operation of the iris recognition system.

Hollingsworth, K. Bowyer and P. Flynn analysis

Recently, K. Hollingsworth, P. Flynn and K. Bowyer described the impact of pupil dilation on iris recognition performance. They discover that when the degree of dilation is similar at recognition and enrollment, comparisons involving highly dilated pupils result in incorrect recognition performance than comparisons involving constricted pupils. They also discover that when the matched images have similarly highly dilated pupils, the mean Hamming distance of the match distribution increases and the mean Hamming distance of the non-match distribution decreases, bringing the distributions closer together from both directions. They further discover that in recognition time matching enrollment and recognition images of the same person,

larger differences in pupil dilation cause higher template dissimilarities, and false non-match.

According to their results, they advise that a measure of pupil dilation be saved as meta-data for every iris code. In addition, the absolute dilation of the two images and the difference in dilation between them should be a reliable measure for matching the iris.

Non-linear Normalization Model for Iris Recognition

X. Yuan and P. Shi proposed a model for normalizing the iris of the eye to recognize the iris of the eye, which combines linear and nonlinear methods of unfolding the iris region. First, nonlinearly convert all iris patterns to a reference annular zone with a predetermined λ, which is the ratio of the radii of the inner and outer boundaries of the iris. Then linearly unfold this support annular zone into a block of a rectangle of fixed size to process a subsequence. The normalization model of the iris is provided by a net of minimal wear and tear of the iris, and it is added for the recognition of the iris of the eye. This model demonstrates the nonlinear property of the iris deformation when the size of the pupil is changed.And experiments show that it is better than a simplified model of linear normalization and improves the performance of iris recognition.

Nonlinear Iris Deformation Correction Based on Gaussian Model

Z. Wei, T. Tan, and Z. Sun introduced a new algorithm for counteracting elastic deformation of the iris.
In the proposed algorithm for non-linear stretching of the iris at any point in the iris region to the pupil's boundary, it is also treated equally with linear stretching plus additive deviation.
The Gaussian function is used to model the deviation. In this algorithm, the images of the iris are corrected by the deviation of the additives between nonlinear and linear stretching of the iris.
Their proposed algorithm for correcting the deformation of the iris allowed more EER as compared to the other two methods of linear and nonlinear normalization. This algorithm gives good results when the pupil dilation causes a nonlinear deformation of the iris, but when the deformation of the iris is linear, this algorithm gives negative results or we need to know the type of deformation of each.

3.4 Previous Research in Analyzing Iris Code

Most researchers identify texture distortions that distort the texture of the appearance, but only a few works on the analysis of bits of the code of the iris and determine which of them are the best bits or unmatched bits. There are very few works in this subject. Iris codes are displayed in this section.

K. Hollingsworth, K. Bowyer and P. Flynn Studies on Iris Code

In the first published work, the consistency of the various bits in the iris code was studied-the paper of K. Hollingsworth, K. Boyer, and P. Flynn. Their experiments proved the existence of fragile bits. They found that all subjects had three different regions that manifested in their iris codes: areas consistently equal to 0, regions consistently equal to 1, and inconsistent areas. Inconsistent regions tend to meet at the boundary between the regions of zeros and regions of the unit. If it was for 30% of the time, then they would say that the bit is transmitted in 30% of the codes of the iris. If the bit was zero most of the time, but one for 30% of the time, they still said that the bit-flipped in 30% of the iris codes. In their study, they found that, on average, 15.99% of the bits in the iris code were perfectly consistent; That is, 15.99% of the unmasked bits were always equal to 0 or always equal to 1, for all iris code of the iris. The subject with the smallest fraction had 4.74% of bits, absolutely matched, and the subject with the largest share had 33.9% bits perfectly matched. They also found that none of them is a difference in the bits of the iris code.

The method of detection of signals Iris Texture S. Ring and K. Bowyer

K. Boyer and S. Ring suggested that some local iris texture distortions were not detected at the segmentation stage and that they generate the corresponding distortions in the iris code obtained from the images. Therefore, they represent an approach for detecting such situations in the rainbow coder through analyzing the results of matching the iris code. Unlike existing sources, to detect local distortions in the texture of the iris, it focuses on analyzing images of the iris of the eyes. On the contrary, their approach to detecting local distortions of the iris texture on images of the same iris focuses on the analysis of the results of the iris code matching. The advantage of this approach is that in it there is only that which can affect the local distortion of the texture of the iris. In addition, this approach can be useful in combination with any improved iris segmentation algorithm. This is the first work

that detects distortions in the texture of the iris, analyzing the results of matching the iris code.

Minimize the Number of Iris code bits needed to Recognize the Iris

K. Frederiksen, G. Dozier, D. Hopes R. Meeks, K. Bryant, M. Savvides and T. Munemoto use the concept of fragile bits and demonstrate how to use the concepts of bit inconsistency and genetic search to minimize the number of Iris Code bits , Necessary for the recognition of the iris of the eye. In addition, they compare two systems: GRIT-I (genetically improved iris templates I) and GRIT-II. Their results show that GRIT-I (the development of the bitmask of the iris) has made it possible to reduce the number of bits of the iris code, which is an average of about 30%. GRIT-II, on the contrary, optimizes the bit mask, as well as bits of the iris code, which have a 100% sequence and 100% protection from the set of training. GRIT-II managed to reduce the number of bits of the IRIS code required by about 89%.

Chapter4Background

This chapter introduces the basic concepts associated with recognizing the iris of the eye and some of the methods used in the proposed algorithms. First, we review the K-averages clustering algorithms. This is followed by the circular transformation of Hough and the Canny edge detection. Finally, morphological operations are described.

4.1 Image K-means Clustering

The K-averages algorithm is an iterative method that is used to split an image into k clusters, assigning to each point a cluster whose center (also called a centroid) is the closest. The center shows the average value of all points in the cluster, in other words, the coordinates are the arithmetic mean for each dimension separately for all points in the cluster. The K-means algorithm we use:

1. Calculate the intensity distribution (also called the histogram) of the intensities.

2. Initialization of centroids with k random intensities.

3. Repeat the next steps until the image cluster labels are no longer changed.

4. Group the points based on the distance of their intensities from the centroid intensities.

$$c_{(i)} := argmin_j || x^{(i)} - \mu j ||^2$$

5. Calculate a new centroid for each clusters.

$$\mu_i := \sum_{i=1}^{m} \frac{\sum_{i=1}^{m} 1\{c_{(i)} = j\} x^{(i)}}{\sum_{i=1}^{m} 1\{c_{(i)} = j\}}$$

Where I sort by all the intensities, j passes through all the centroids, and μ_i- the intensity of the centroids.

The distance is the absolute difference between the pixel and the center of the cluster. The distance in our algorithm usually depends on the intensity of the pixels. To group K-tools, you need to specify the number of clusters to be broken and the distance metric to determine how two objects are closed to each other.

4.2 Circular Hough Transform

It is an image transformation that allows you to extract circular objects from an image, even if the circle is incomplete. It can be described as the point transformation in the x, y plane into a parameter space. The parameter space is determined in according to the shape of the interested object. The circle is really simply represented in the parameter space in comparison with other forms, since the parameters of the circle can be directly transferred to the parameter space. The circle equation is r2 = (x-a) 2 + (y-b) 2. As you can see, the circle has received three parameters a, b and r. Where a and b are respectively the center of the circle and r is the radius of circle. The parametric representation of the circle is

$$x = a + r \cos(\theta)$$

$$y = b + r \sin(\theta)$$

The space of parameters for the circle will belong to R3, whereas the line will belong to R2 only. Since the number of parameters necessary to describe the form increases, and the dimension of the parameter space R increases, then the complexity of the Hough transformation is also. The circular Hough transform can be used to determine

the radius and coordinates of the center of the pupil and iris region. The locus of points (a, b) in the parameter space falls onto a circle of radius R with center (x, y). The true central point will be common to all the circles of the parameters and can be found with the accumulation array Hough. Figure 3.1 shows this process.

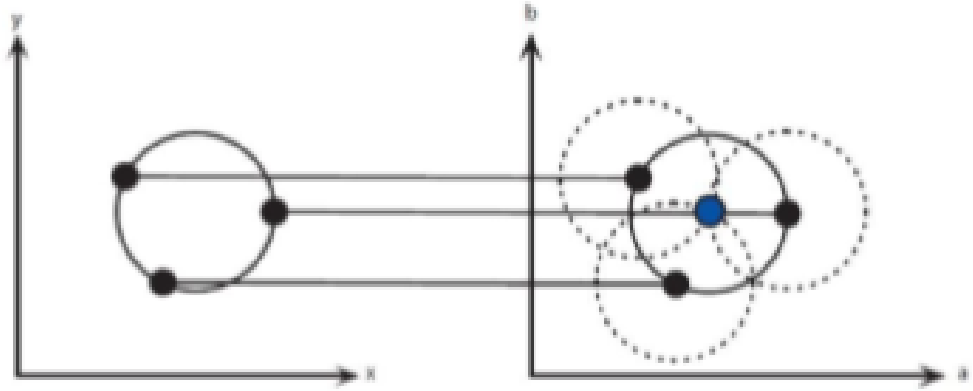

Figure 4.1:Graphicrepresentation of circular Hough transformation

In the coordinates that belong to the drawn circle perimeter, we increase the value in our battery matrix, which is essentially equal to the size of the parameter. Thus, we run each point of the edge in the input circles of drawing the image with the desired radius and increase the values in our accumulator. When all the boundary points and each desired radius are used. The accumulator will now contain numbers corresponding to the number of circles passing through individual coordinates. Thus, the highest numbers (chosen in a reasonable way, relative to the radius) correspond to the center of the circles in the image.

4.3 Canny Edge Detection

There are many methods for detecting boundaries, but one of the most ideal methods for edge detection is the Canny edge detection. It receives an image in grayscale and outputs a binary map corresponding to the identified edges. It begins with a blur operation behind a gradient map for each pixel in the image. In the non-maximum suppression step, a value of 0 is set for all gradient map pixels that have neighbors with higher gradient values. In addition, in the hysteresis process, two predefined values are used to sort some pixels as boundary or without edges. Finally, the edges expand recursively to those pixels that are neighbors of other edges and with a

gradient amplitude above the lower threshold. Canny edge detection takes the following arguments:

Upper threshold: this parameter is used in the hysteresis operation. Sets higher gradient map values for viewing as edge points.

Lower threshold: this parameter is used in pixels with hysteresis mode, the values of the gradient below which are considered non-edge points.

Sigma of a Gaussian kernel: this parameter determines the standard deviation of a two-dimensional Gaussian kernel. Higher values increase the power of the blur operator and lead to a smaller number of detected edges. Weight of vertical faces: used for weighting vertical derivatives in a gradient map. It is usually in the interval and multiplied by the value of the vertical derivative.

Weight of horizontal faces: similar to the above parameter, it is a correspondent for horizontal derivatives. It should be noted that usually the sum of the vertical and horizontal weight values should be equal to 1.

Scaling factor: This factor is used to reduce the image size to reduce the number of edge points.

These arguments are defined according to applications and environments that use the Canny edge detection. In the fourth chapter.

4.4 Morphological Operations

Morphological processing refers to certain operations when an object falls on a structuring element and is reduced to a more revealing form. The goal is to convert the signal into a simpler one by removing redundant information and apply to binary and gray signals. Most morphological operations can be defined in terms of two mainoperations: erosion and dilation. Erosion and dilation are two morphological operations that are very necessary in processing binary images. Erosion and dilation allow groups of units represented by white pixels to be grouped to increase or decrease to obtain resulting images that either fill the gaps of the grouping, or remove small groups of them as needed. Erosion is best described as a mathematical operator, which reduces the grouping of units in binary images. A structuring element or a kernel represented by a matrix of ones and zeros is transmitted through the original

image. During erosion, the resulting image is a collection of all the originating points of the structuring element in which the translated structuring element does not overlap with the background of the original image. The eroded image of the image I with respect to the structuring element S is the set of all support points x for which S is completely contained in I:

$$I \ominus S := \cup\{x : S + x \subset I\}$$

Ultimately, small groupings of ones and thin lines are removed from the image.

A dilation is a mathematical operator that extends groupings of units, filling in holes or gaps in a binary image. Dilating the image with the structuring element results in a mapping consisting of all the initial locations of the structuring element, where the reflected and translated structuring element overlaps at least some of the image. The dilated image of the object I with respect to the structuring element S is the set of all reference points for which S and I have at least one common point:

$$I \oplus S := \cup\{x : S + x \in I\}$$

When the binary image is repeatedly dilated, the black space (zeros) within the groupings of ones is eliminated to reach one homogeneous region. On the basis of dilation and erosion operations, the opening and closing of the image is realized. The opening corresponds to the erosion of the image, followed by the dilation of the image, and the closing corresponds to the opposite (image dilation, followed by erosion of the image). In our algorithm of iris segmentation, the goal of using morphological operations is to exclude possible noisy data and smooth information in order to facilitate segmentation.

Chapter 5 Proposed Algorithms

5.1 Proposed Iris Recognition Algorithms

In this thesis, we propose three methods for improving the iris recognition system. As shown in Figure 5.1, the first segmentation algorithm for processing images of the iris was captured under less restricted conditions. This algorithm reduces the percentage of errors, while there isnoise, such as specular reflection and iris barriers. The proposed algorithm begins with the determination of the expected area of the iris using the K-average clustering algorithm, then a circular Hough transform is used to localize the iris boundary, after which some algorithms are proposed for detecting and isolating noise regions.

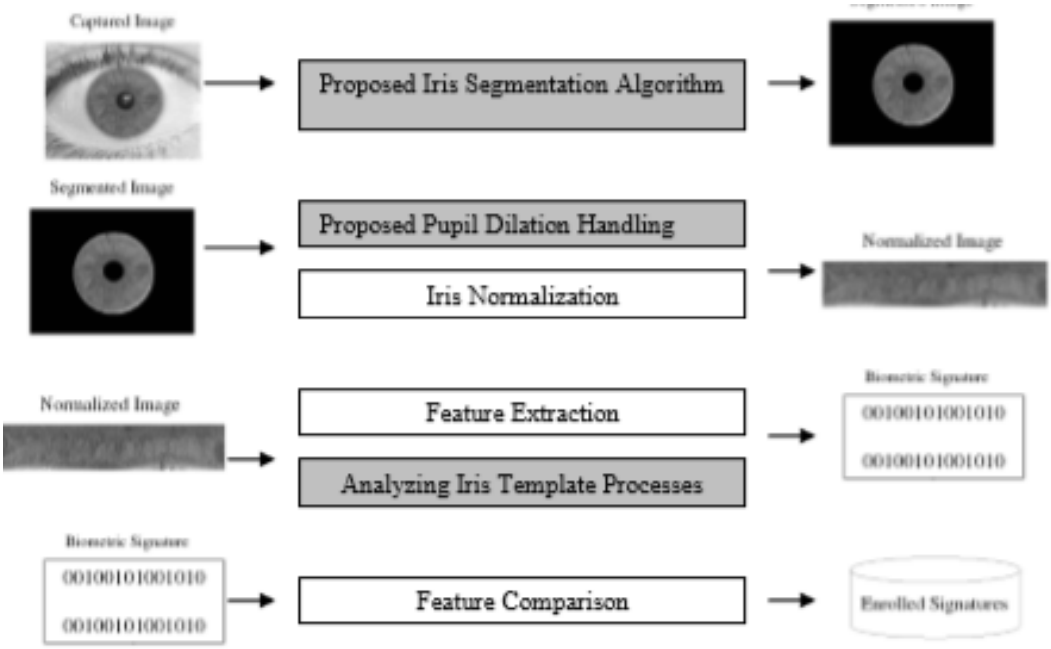

Figure 5.1: Block diagram of proposed improved iris recognition algorithms, gray rectangles represent our own work

In the second method, the effect of pupil dilation on the iris recognition system is studied to show that the degree of high dilation of the pupil degrades the iris pattern and affects the work of the recognition system. After this, the limit of the dilation degree is determined, which after it affects the iris code or some of its information will be declined. This limit can be used to prevent unwanted dilatation of the pupil.

Finally, we analyze the iris code bits to determine the matched and mismatched bits, and we compare the inner and outer regions to find which area contains the more inconsistent bits that should be excluded from the iris pattern.

5.2 Proposed Iris Segmentation Method

This section deals with one of the most important steps in the construction of the iris recognition system, which is the iris segmentation. At this stage, we must accurately extract the area of the iris, despite the presence of noise, such as the alter sizes of the pupil, shadows, specular reflections and glare. The segmentation step is important, because it underlies all further operations, such as normalization and coding. As already mentioned, there are many iris segmentation algorithms that were proposed earlier and gave excellent results when iris images were selected in a near infrared camera and under ideal imaging conditions. The accuracy of modern segmentation algorithms is significantly reduced when working with noisy iris image taken at a visible wavelength, under far from ideal imaging conditions, for example, in the UBIRIS.v1 and v2 database. Our main motivation in this section is to offer a new segmentation algorithm for processing images of the iris in less constrained conditions.

As already mentioned in the third chapter, the methods of segmentation can be divided into two categories. The first category applies a certain type of operators, such as the Daugman‘s integrodifferential operator, and usually these operators are affected by noise and separability between the iris and the sclera. In the second category, one type of edge detection filter is used, such as the Canny or Sobel edge detection, followed by circular Hough transformation, and these methods are usually very expensive in time.

Our main goal in this section is to develop a reliable iris segmentation method that does not depend on the types of noise and at the same time is not expensive in time. As shown in the experiments in Section 5.3, our proposed segmentation algorithm significantly improves the reliability of the segmentation process even for large noisy iris regions. In Fig. 5.2 is a block diagram of the segmentation algorithm proposed by us.

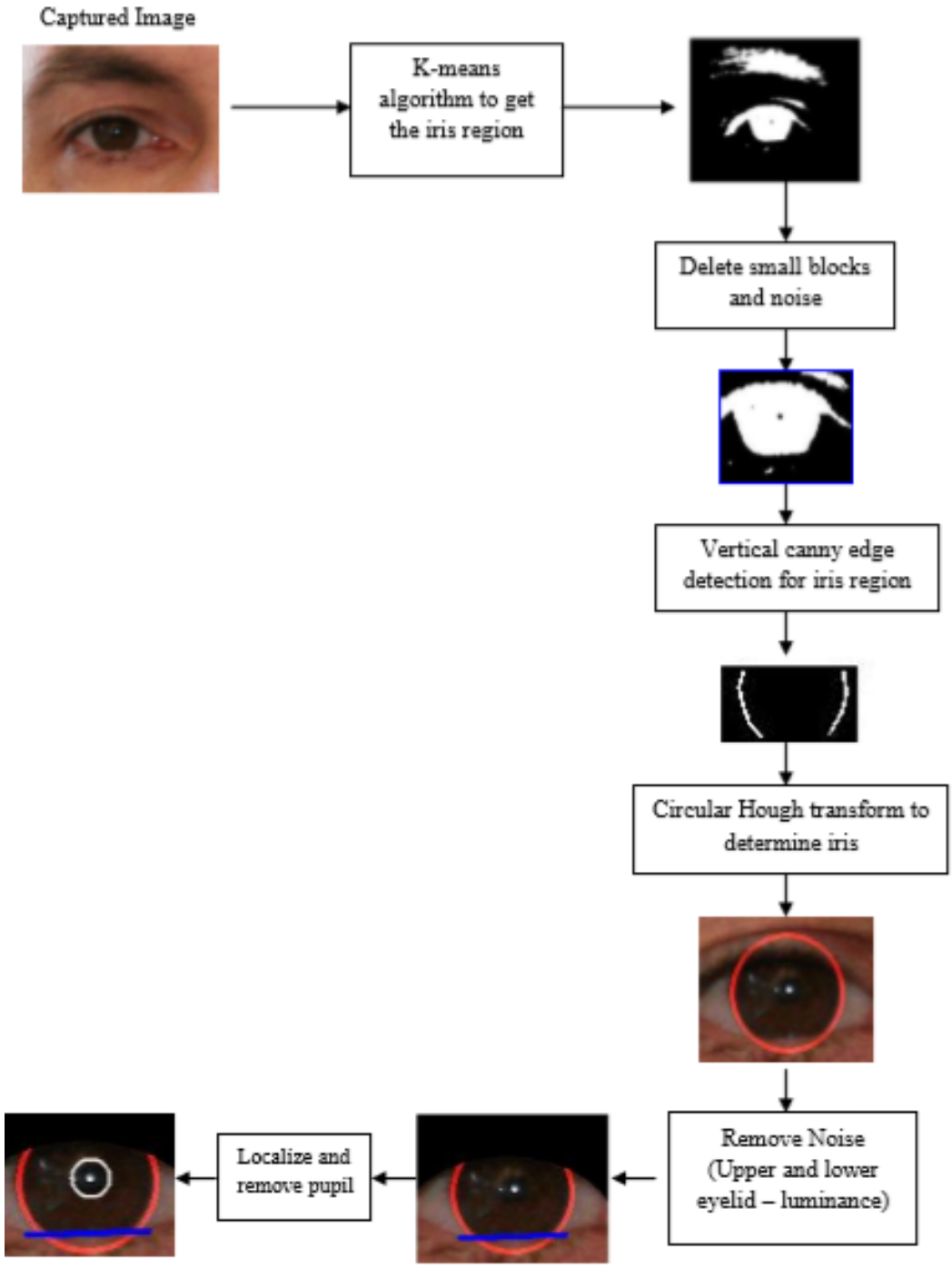

Figure: 5.2 is a block diagram of the segmentation algorithm

Algorithm 5.1 shows the steps of our proposed iris segmentation algorithm.

Purpose Segment of noisy irises. Input: Iris image. Output: Segmented iris without noise

Procedures:

Step 1: Determine the expected area of the iris using the K-averages algorithm. A) Separate the red color space from the color space of the RGB image. B) Apply the image clustering algorithm, as described in Section 3.1, with the number of clusters equal to three, and the distance - the intensity of the pixels. C) Select a cluster with a low intensity (Dark area in the image). D) Remove small blocks and noise.

Step 2: Apply the edge detection algorithm. A) Convert the RGB color space of the expected area of the iris into the YCbCr color space and separate the Y component. B) Reduce the image scaling factor to 0.5. C) Apply Canny edge detection. D) Remove the small noise components by applying some morphological operations.

Step 3: Use the circular Hough transform explained in section 3.3 on the binary edge image and select the maximum parameters group (a, b, r) from the accumulator, then find the Cartesian parameters (x, y, r) that are the center coordinates and the radius of the iris.

Step 4: Localization of the upper eyelid. A) Isolate two small rectangles on both sides of the outer iris. B) Apply horizontal detection of the Canny edge to these two small rectangles and isolate the noise using morphological operations. C) Determine the coordinates of the upper eyelid on both rectangles. D) Draw an arc that passes through two coordinates of the upper eyelid on each rectangle, and the radius is twice the radius of the iris.

Step 5: Localization of the lower eyelids. A) Take edge map of the lower half of the iris. B) Find the optimal line fit by line Hough transform. C) If the vote on the line is less than a certain value, then we do not assume that the occlusion of the lower eyelid occurs.

Step 6: Isolate specular reflections. A) Calculate the average intensity in the three RGB color spaces for the iris area. B) If the intensity of each pixel is greater than the average intensity computed in the first stage plus a constant value (explained in more detail below), then we consider this pixel as a pixel of reflected noise.

Step 7: Delete the pupil area. A) Adjust the iris image by matching the intensity values of its bits with the new values to focus on dark intensities. B) Filter the image with the median filter. C) Canny edge detection is used to obtain a rib map. D) The

circular transformation of Hough is used to localize the pupil, suggesting that it is circular.

The proposed segmentation algorithm avoids the launch from the pupil, since the pupil is not always the darkest region of the eye in noisy images that were shot at the visible wavelength (due to certain factors, such as shadows, specular reflections and glare). In Fig. 5.3 shows some noisy images of the eyes in which the pupil experiences the influence of these factors. Also, we avoid running our algorithm from the sclera, because sometimes the sclera is covered with dark colors, and these dark colors cause errors in determining the area of the iris, and as a result, the segmentation process will be incorrect. Figure 5.4 shows an example of an unclear sclera that will affect the results of segmentation.

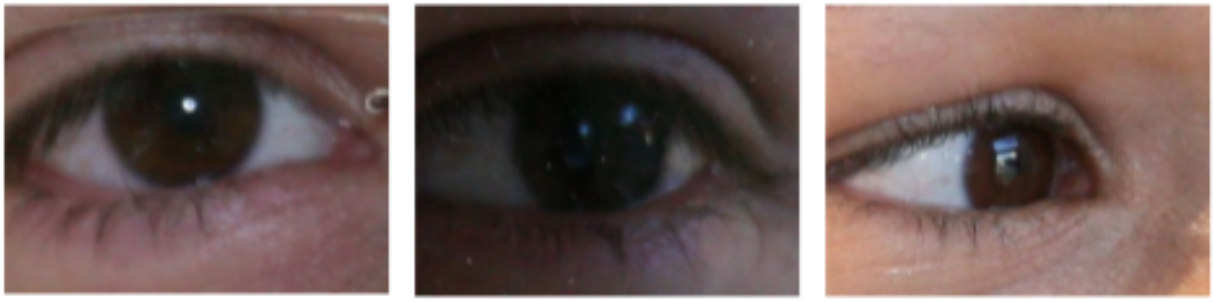

Figure 5.3: Noisy images of the iris selected from the UBIRIS v2 iris database. The pupil reflects mirror reflections and glare on the first and third images. The second image shows a pupil affected by poor brightness and shadows.

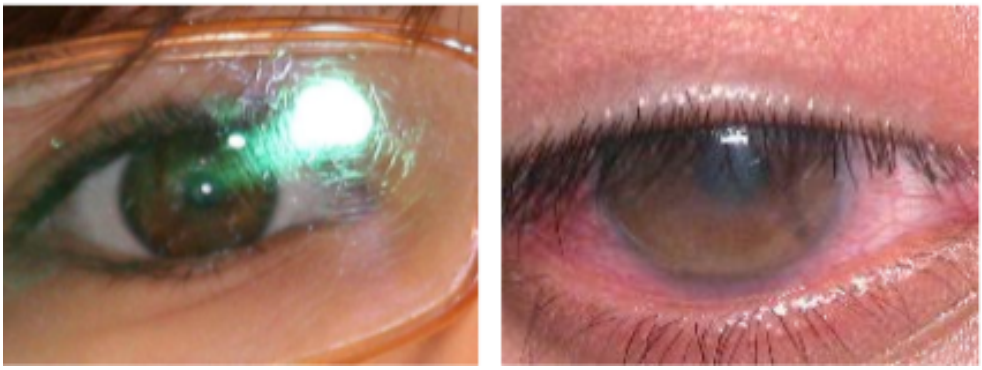

Figure 5.4:Noisy images selected from the UBIRIS v2 and v1 iris databases, respectively. On the first image, there are more white spots than sclera, and on the second image sclera are covered with dark colors.

The proposed segmentation algorithm starts with determining the expected area of the iris using the K-means clustering algorithm. The output image is used by vertical detection of the Canny edge to create edge maps. The circular Hough transform is applied to the edge image to determine the supposed center and radius of the iris. We use K-means of clustering and vertical edges of the map to shorten the time of searching for the circular transformation of Hough. Therefore, the circular Hough transform will be applied to the binary edge image, which results from applying edge detection on the mask of the region that is the result of the K-means. After determining the circle of the iris, we apply some new methods to isolate noisy factors such as eyelids, eyelashes, brightness and reflections. Finally, we remove the pupil area from the iris area.

5.2.1 Determining Iris Region

One of the main causes of segmentation errors is high local contrast (for example, on eyelashes, eyebrows, glass frame or white areas due to brightness on the skin beyond the eye region) occurs in non-iris region. Therefore, it is recommended to avoid such segmentation errors, excluding non-iris region in the image of the iris before the step of localization of the iris. Obviously, if we can divide the image of the iris into three areas like the iris, the skin area and the sclera region, then we can reduce segmentation errors and at the same time reduce the search time in the next stages of the segmentation process.

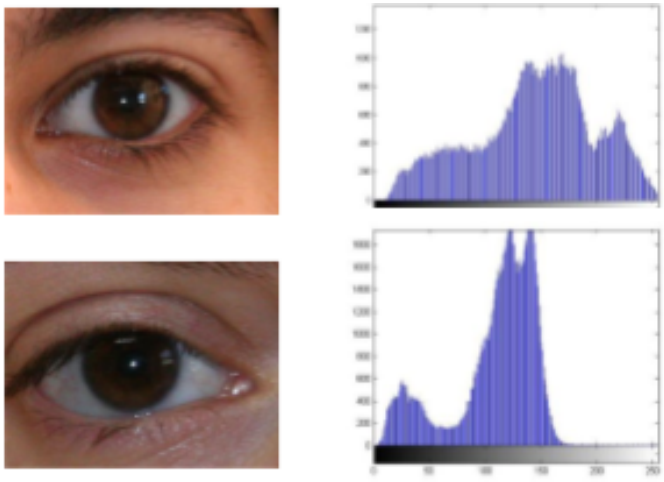

Figure 5.5:The histograms of two eye images from UBIRIS database.

A simple clustering method is proposed for dividing the image of the eye into three different parts based on clustering of K-means. The image of the eye can be divided into three areas. The first area, having small values of intensity, consists of the iris (including the pupil) and the eyelashes. The second region, which has high intensity values, consists of a sclera and some glare or reflections of brightness. The third area is the area of the skin, its intensity between the two previous regions. Figure 5.5 shows a histogram of two images of the iris. In Fig. 5.5, three local maxima can be seen that represent areas of the eye images. If we classify the image into four clusters, the iris area on the images with the light color of the irises (for example, blue and green irises) will be reduced, and the segmentation process will not succeed. This is due to the fact that the border of the iris can lie outside the area of the iris. Although, if we divide the image into two clusters, the area of the iris becomes wider, usually more than half the image area. This will add the non-iris areas to the iris area, which will cause errors and will increase the execution time of the Hough transform in the next step. The K-means clustering algorithm is effective, because it deals only with the darkest region, and we will not worry about the other two clusters. As mentioned in the reference chapter, the K-means algorithm is an iterative method that is used to split an image into K clusters, assigning each point to a cluster whose center (also called a centroid) is the closest. The center shows the average value of all points in the cluster, in other words, the coordinates are the arithmetic mean for each dimension separately for all points in the cluster. The distance is the absolute difference between the pixel and the center of the cluster. The distance in our algorithm usually depends on the intensity of the pixels. For clustering of K-means, it is required to experimentally indicate the number of clusters to be partitioned experimentally that at K equal to three the algorithm gives the best results.

First, we separate the red color space from the RGB image color space, since it contains most of the iris details. Then we apply the K-means algorithm for clustering the image, as described in Chapter 4, in the red color space of the image. After clustering, the resulting image is processed by some morphological operationsto remove small blocks and noise. We select the closest block from the center to drop the eyebrow area. Figure 5.6 shows the result when we apply the clustering algorithm for some images. White areas represent the darkest area (which is the area of the iris and eyelashes) in the image. Black areas represent the sclera area and some glare or reflections of brightness. Gray areas - this is the area of the skin, the intensity of

which is between the two previous areas. As can be seen in Figure 5.6, the white area covers the iris, eyelashes, and sometimes the eyebrow, but excludes brightness and specular reflections. This is very useful for reducing the areas being treated. The clustering algorithm reduces the area of the iris by more than 70%. Therefore, the search time for the next steps will also be reduced.

a)

b)

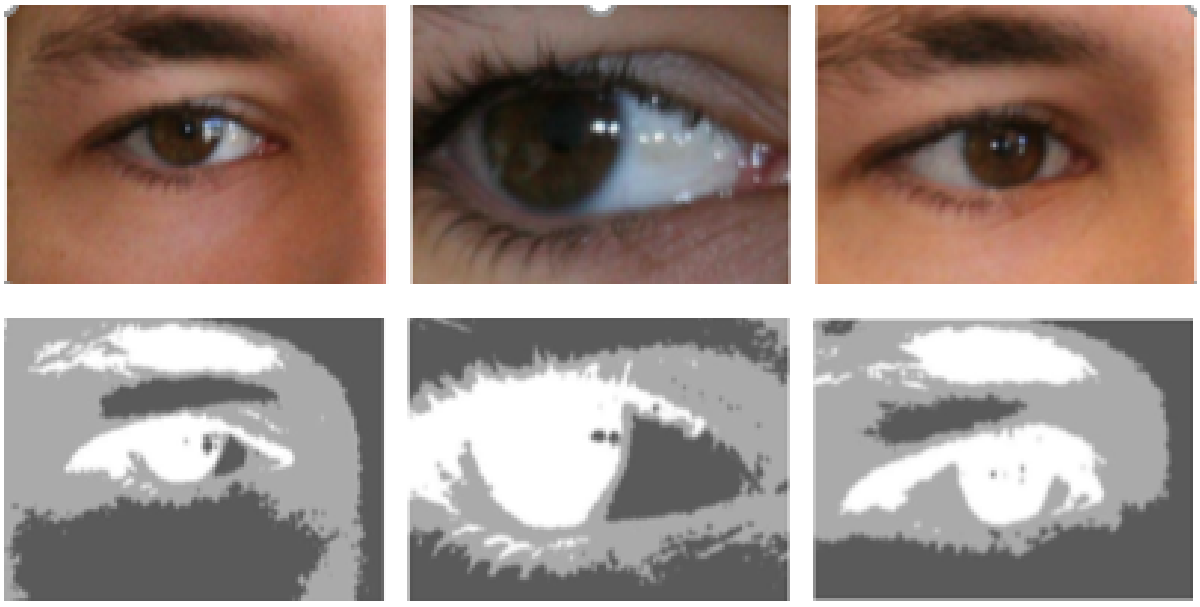

Figure 5.6:Illustration of the results of K-mean clustering on some images (a) real images. (b) Clustering result images, white regions represent the estimated iris region.

5.2.2 Edge Detection

To find the boundary points in the iris image, use the Canny edge detection as described in Section 4.3. The implemented Canny edge detection has six arguments. We set the upper threshold and lower threshold inputs experimentally to make the algorithm suitable for the noisy iris images.In our algorithm, to select the border of the iris-sclera, we choose a high value for the weight of the vertical edges and a low value for the weight of the horizontal edges, because we are only interested in vertical edges. These values are regulated only once for the entire database (to match the environmental conditions) and do not need to be calculated for each image of the iris. This process reduces the number of errors caused by horizontal edges caused by eyelashes and eyelids. The zoom factor is 0.5 to reduce the image size to half. This reduction in scale will reduce the required pixels to half. We found that if we reduce

the scale factor to less than 0.5, many edge points will disappear, leading to errors in the localization of the iris border.

In our algorithm, we did not use the image in grayscale as input. Instead, we experimentally discover that the best used image is the Y component of the YCbCr color space. First, we convert the image from RGB to the YCbCr color space, and then the Y component is split. Finally, the median filter is applied to the image of the Y component for processing small noises and smoothing the image. Remember that edge detection, applied only in the reduced area, is the result of the clustering step. Figure 5.7 shows the results of applying Canny edge detection on sample images. Figure 5.7 (b) shows the Y component of the YCbCr color space, we notice that this component reduces the effect of brightness, specular reflection and red areas in the sclera. As a result, more edge points can be avoided in order to process them in the “Circular Hough Transform"(CHT) step. Figure 5.7 (c) shows images after applying the Canny edge detection, we see that the largest two related components are the iris boundaries, but the amount of small noise components still exists. We can reduce the amount of small noise components by applying some morphological operations. The result is shown in Figure 5.7 (d). Although there are noise components, we reduce the boundary points that will be processed or searched by CHT in a very good method. We note that the images of binary edges in Fig. 5.7 (c) and (d) are scanned 0.5 times after scaling. Also, to reduce the edges that will look for CHT as much as possible.

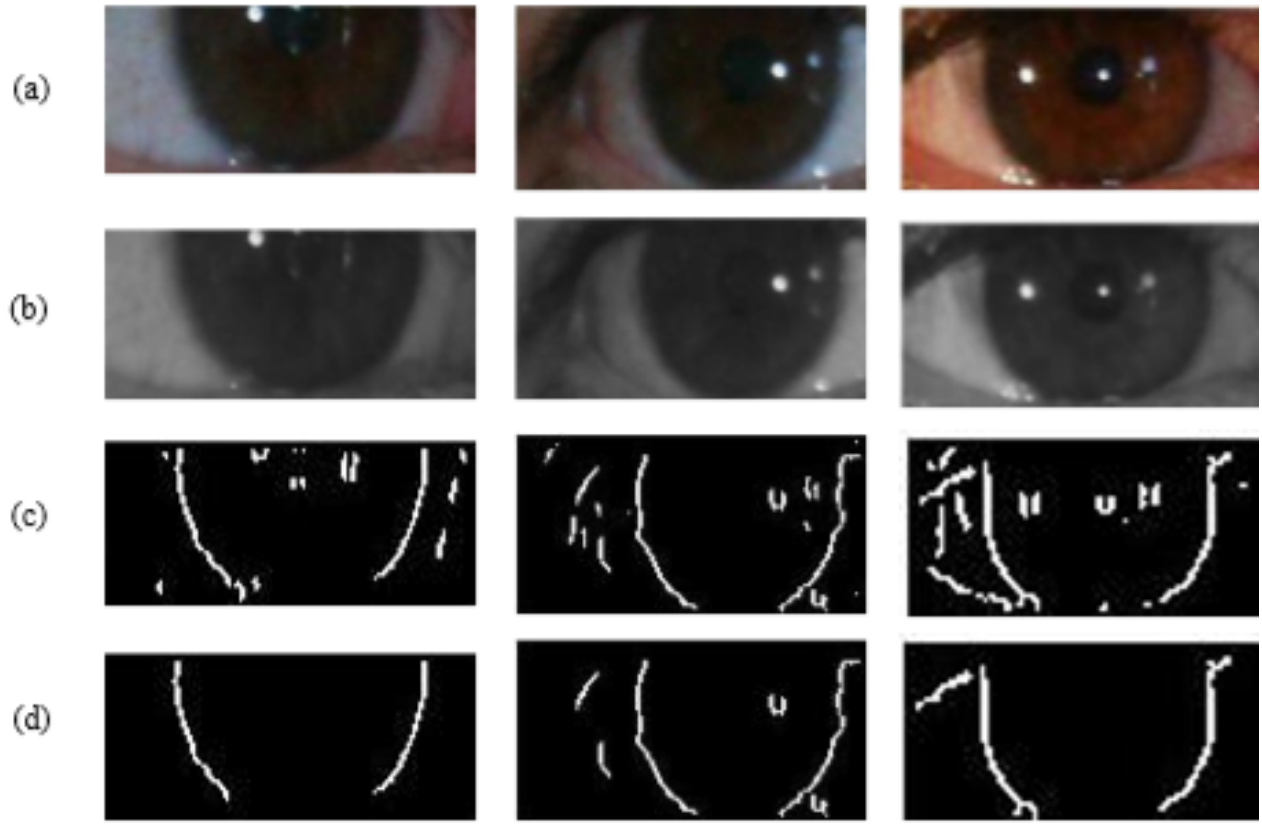

Figure 5.7: Illustration of Canny edge detection application results on some images (a) real images are the result of a clustering step. (B)Y component of the image after conversion to the YCbCr color space. (c) A binary image is obtained from the detection of the Canny edge using a scaling factor of 0.5 (d) Binary image after removing small blocks and noises.

5.2.3 Circular Hough Transform

As mentioned in the fourth chapter, the circular Hough transformation belongs to the space R3, so the complexity of the Hough transformation is O (n3). Therefore, in order to shorten the execution time, we use three methods that were explained in the previous steps:

1. Scale factor: reduces the size of the image and reduces the edges.

2. K-means clustering: reduce the search area and reduce the edge points when using the Canny edge detection.

3. Using morphological operations: removing small blocks and noises in the binary edge image.

After application of a circular Hough transform, described in Section 3.3, a binary edge image, we choose the maximum group of parameters (a, b, r) of the battery, and then find the cartesian parameters (x, y, r), to define the iris on image. In Fig. 5.8 shows some examples.As shown in this figure, the boundary of the iris location is detected, and the white circles adjust irises accurately, despite the presence of some noise factors, such as specular reflections, iris occlusion and eyelashes. In addition, we notice that irises are localized correctly regardless of their size, this is another advantage of our segmentation algorithm.

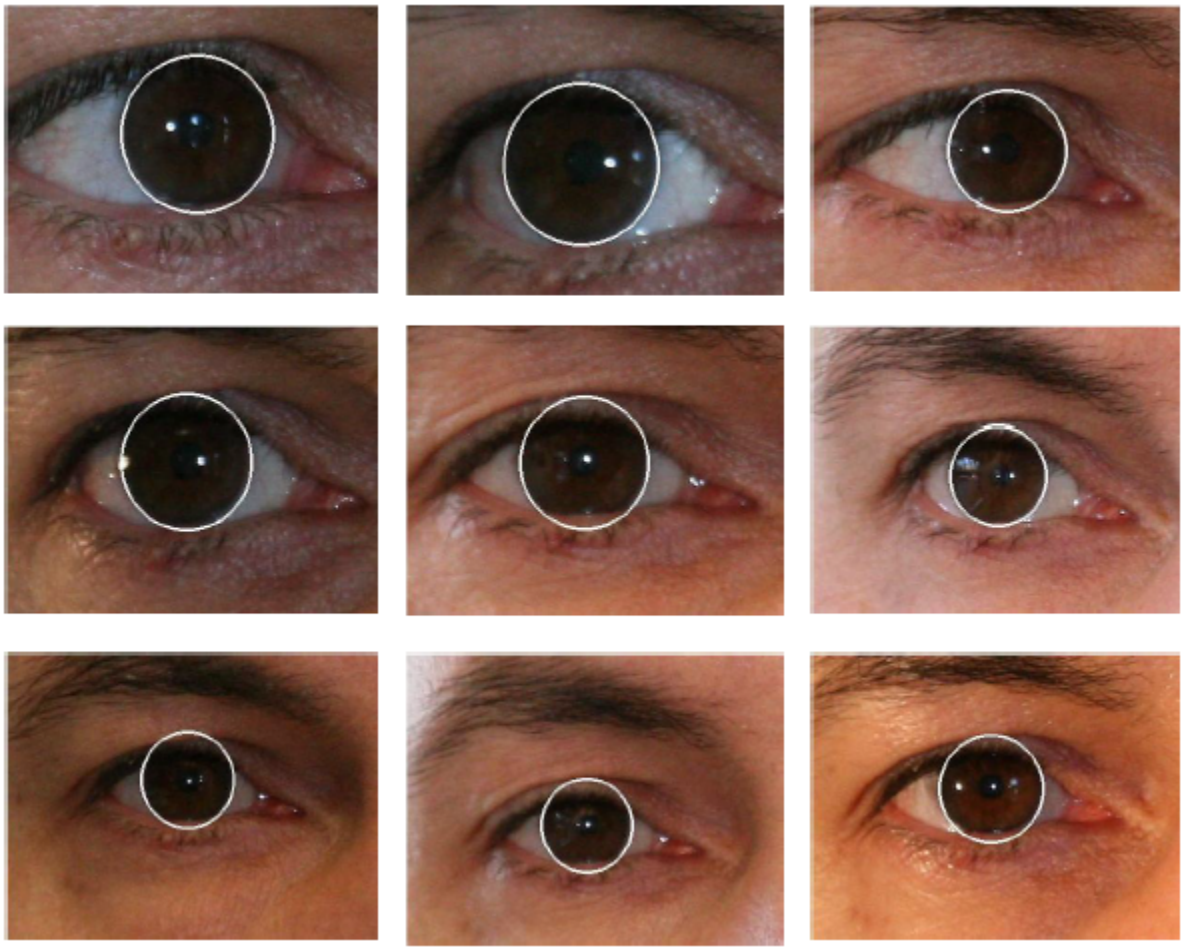

Figure 5.8: Samples of segmented irises from UBIRIS v2.

5.2.4 Isolating Noise

In non-cooperative recognition of the iris, the user has little or no participation in the process of image capture. As a result, images of the iris are often captured with more noisy artifacts, such as reflections, eyelid or eyelid occlusions, shadows, etc. It is

reported that most localizations fail occur on non-iris areas due to high local contrast. Therefore, in order to avoid such localizations, we must exclude non-visual areas and process all sources of errors. In this subsection, we explain how the proposed segmentation method handles each of them.

Localization of the upper eyelid.

Researchers use a variety of methods to localize the eyelid of the iris(for example, edge detection, an integrodifferential operator and the line Hough transformation) that are captured in ideal environments. Therefore, these methods are ineffective for use in images of noisy iris, since the intense contrast of the iris and eyelids can be very low, especially for heavily pigmented (dark) irises, as shown in Figure 5.3. We propose a new method of localizing the eyelids, determining it in the sclera region. We determine the eyelids in the sclera, because the intense contrast between the sclera and the upper eyelid is very high than the intense contrast between the iris of the eye and the upper eyelid. The following steps explain the algorithm of localization of the upper eyelid.

a) Isolate two small rectangles from the two outer sides of the iris. Each of them starts vertically from the center of the iris and expands to a value greater than the center of the iris, as shown in Figure 5.9.

b) apply any type of a horizontal edge detection on two rectangles (for example, Canny edge detection) and isolate the noise using some morphological operations.

c) Determine the coordinates of the upper eyelid on both rectangles. Assuming that this is the largest horizontal edge line on each rectangle.

D) Draw an arc that passes through the two coordinates of the upper eyelid on each rectangle, and the radius is twice the radius of the iris. The arc center is calculated using the following steps.

Let the coordinates of the upper eyelid on the first rectangle be equal (x1, y1), and the coordinates of the upper eyelid on the second rectangle be (x2, y2). The line passing through the two coordinates of the upper eyelid on each rectangle is given by the equation:

$Ax + by + c_{horii} = 0$

where

$$a = y2 - y1,\ b = x1 - x2,\ c_{hori} = x2y1 - x1y2 \ldots\ldots\ldots (4.1)$$

Let (p, q) be the midpoint of the horizontal line joining (x, y1) and (x2, y2). Then the equation of the perpendicular to the horizontal line at the midpoint of two points (x1, y1) and (x2, y2):

$Bx - ay + c_{vert} = 0$, where $c_{vert} = aq - bp$. Then we find the point lying on the vertical line and at a distance of double iris radius from the middle of the horizontal line, as

shown in Figure 5.9.

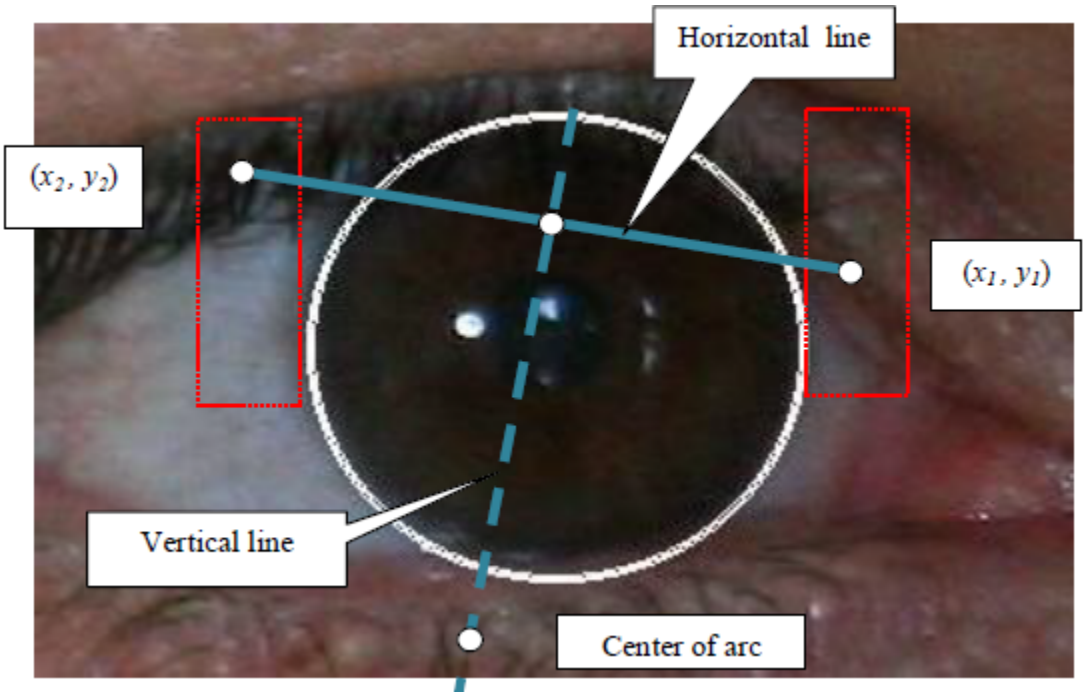

Figure 5.9: Upper eyelid localization model**.**

Figure 4.10 shows the samples of UBIRIS v2 and v1 after using our method to localize the upper eyelid of the iris. Note that, using the arc in the proposed method, the iris area will not lose the area without noise, as it happened when using the Hog Line transformation. Figure 4.10 shows that our algorithm accurately isolates the upper eyelid, even if the intensity of the iris contrast and the eyelid is very low and cannot be isolated by conventional processes, such as the Hough transform or the Daugman Integrodifferential operator. The effectiveness of our algorithm is explained by the use of contrast intensity between the sclera and the upper eyelid, rather than the iris and the upper eyelid. In addition, we can see that this algorithm still works when the huge area of the iris is closed by the upper eyelid.

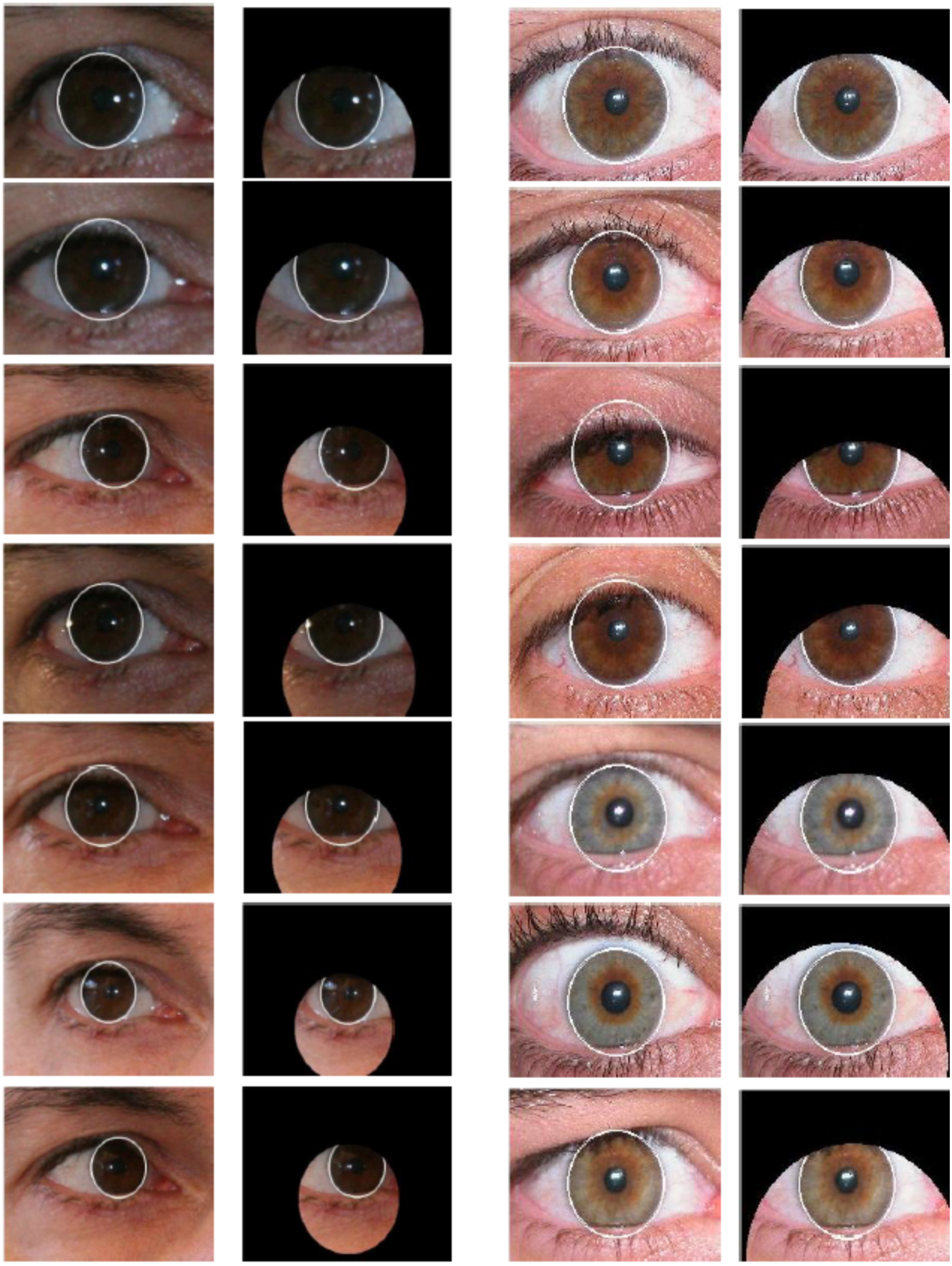

Figure 5.10: Algorithm for localization of the upper eyelid (a) segmented images from UBIRIS v2. (B) segmented images from UBIRIS v2 after using the proposed localization of the upper eyelid. (C) segmented images from UBIRIS v1. (D) segmented images from UBIRIS v1 after using the proposed localization of the upper eyelid.

Lower Eyelid Localization To localize the iris lower eyelid, we use the line Hough transformation, since most occlusions of the lower eyelid are approximately linear. First, we apply the definition of the Canny edge to the bottom half of the iris, and then the best line corresponding to the Hough line transformation will be found. If the vote of the line is less than a specific value, then we assume that the no occlusions of the lower eyelids occur.

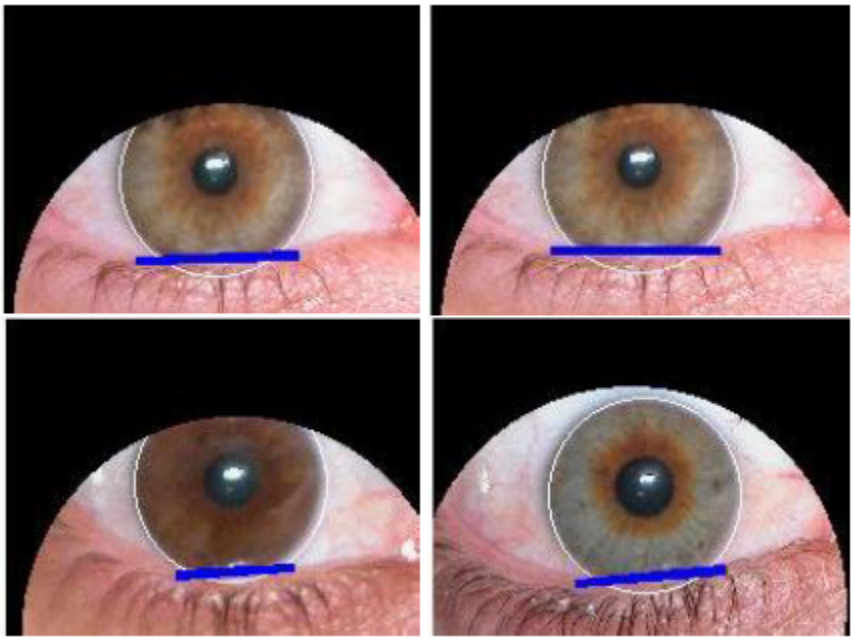

Figure 5.11: Lower eyelid localization samples using UBIRIS v1 database.

Figure 5.11 shows some examples after the localization of the lower eyelid. The blue line represents the largest line of the edge that distinguish the iris and lower eyelid. We notice that the process of isolating the lower eyelids is simpler than the upper eyelid, because there is no occlusion of the eyelashes, and usually the occluded region of the iris due to the lower eyelid is smaller than the occluded area of the iris due to the upper eyelid.

Isolation of specular reflections

If there are noisy images that processed by the iris recognition system specular reflections can be a serious problem. We offer a new simple way to remove reflections in two stages:

1. Calculate the average intensity of the iris area in the three-color spaces of RGB (after removing the upper and lower eyelids).
2. Test the intensity of each pixel in the iris, and if the pixel intensity in a particular color space is greater than the average intensity computed in the first stage plus a constant value, then treat this pixel as a pixel of reflected noise. The value of the constant is adjusted only once for all images.

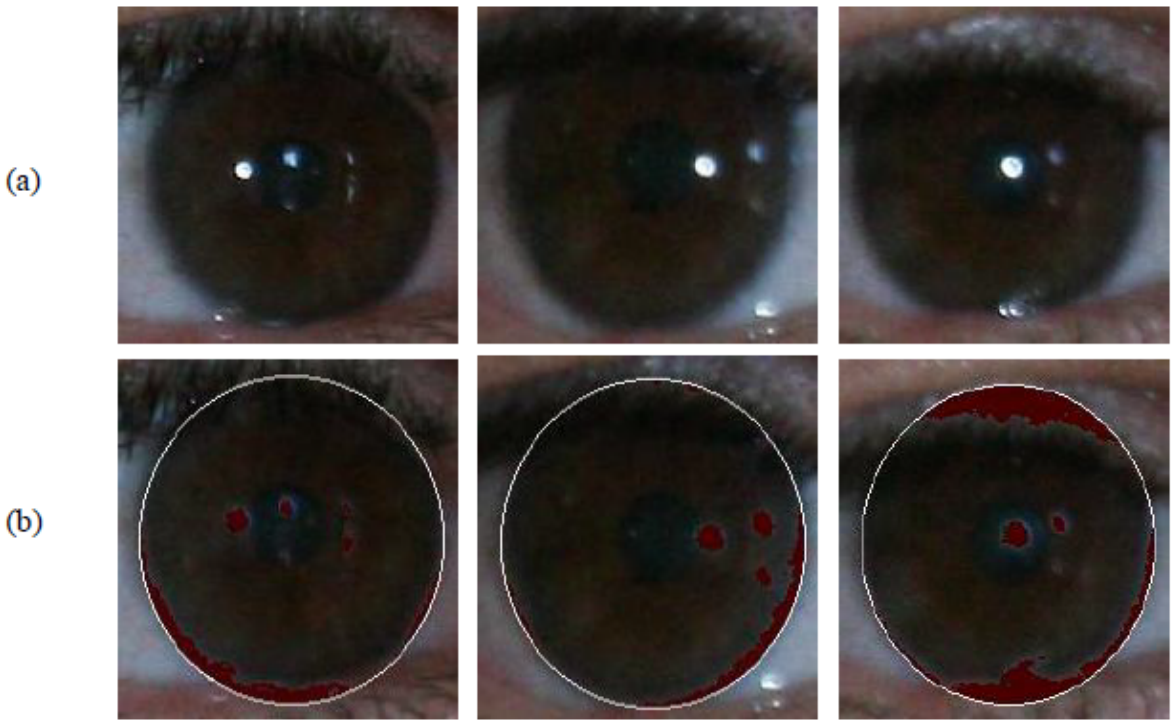

Figure 5.12: Isolation of reflections from iris in the proposed algorithm (a) reflected image. (b) detect areas of reflection (marked in red).

Figure 5.12 looks at some images after mirroring is localized. Pixels that differ in red color are masked for isolation when the iris template code is extracted. We notice that the areas of specular reflection and highlight are precisely defined, even if there is a small area of light or occlusion, as shown in Figure 5.12. Note that this process can also discard some redundant spaces that can be caused from the angle of the selected images.

5.2.5 Removing Pupil Region

The elimination of pupils remains at the last step, since one of the main differences between eye images in noisy databases was captured under visible wavelengths, and with such images obtained in near infrared (NIR) illumination is that the intensity contrast of iris and the pupil is very low, especially for heavily pigmented (dark) irises, as in Fig. 4.6 and 4.9. If we directly try to localize the pupil, we will fail. Therefore, the best way is to increase the iris of the image to make the pupil appear with the method of increasing the contrast. The following steps explain the process of removing the pupils.

a) Regulate the image of the iris, comparing the intensity values of its bits with the new values to focus on dark intensities.

b) Apply the median filter to reduce noise factors and save the edges.

c) Edge detection is used to obtain an edge map.

d) The circular Hough transformation is used to localize the pupil, assuming that it is circular. The pupil radius is set equal to 1/10 of the radius of the iris as the lower limit to 7/10 of the radius of the iris as the upper limit.

Figure 4.13 shows the steps of this algorithm using an image from UBIRIS v2. Note that all the previous steps are applied only on the inner square of the iris to avoid errors that can occur due to the boundary points outside area of the pupil to and shorten the execution time. As we see in Fig. 5.13, the success of pupil localization, even if the contrast of iris and pupil brightness is very low.

Figure 5.13: Steps of the pupil removal algorithm (a) the inner square of the iris. (B) the result of adjusting the image in (a). (C) the result of Canny edge detection. (D) the result of the circular Hough transformation.

5.3 Pupil dilation

Iris recognition systems face many problems, such as eyelashes, eyelids, specular reflections and pupil dilatation. Researchers are very interested in problems that cover parts of the iris or create some noise on it. But only a few researchers are trying to discuss the pupil dilation problem, because the effect of this problem is relatively not obvious to the eye. In the Daugman's early work, the normalization of the iris allows us to compare two images of different sizes. However, information on the degree of dilation of the pupil is discarded. In this section, we show that the dilation of the pupil worsens the iris pattern and affects the work of the recognition system. To show this, the following steps are performed.

Algorithm 5.2: Analysis of the influence of the pupil dilatation algorithm.

Purpose: analysis of the effect of dilatation of the pupil.
Input: Iris images.
Result: Proof that dilating the pupil reduces the effectiveness of iris recognition systems.
Procedures:
Step 1: Assemble the iris image data set that contains many irises for the same class that have widely variations in the dilation degrees of the pupil.
Step 2: segment the irises in the selected data set and code each iris in it to create your iris code.
Step 3: Compare the patterns of all the irises in the dataset with all other iris patterns in the data set.
a) compare irises in one class to generate a distribution of intra-class comparisons.
b) compare irises in different classes to generate a distribution of interclass comparisons.
Step 4: Calculate FMR and FNMR for this dataset.
Step 5: Eliminate irises with an dilation degree of more than 0.5 from the data set and repeat steps from 1 to 4.

Step 6: Compare the results.
As shown in Algorithm 5.2, we compare the error rates for the two sets of data, the first data set contains all the degrees of the pupil expansion. The second set of data contains only irises with a small degree of dilation of the pupil. If pupil dilation affects performance, the error rate of the second set of data should be less than the first data set error rate. In Section 5.2, experimental results show that the dilation of the pupil affects the functioning of the iris recognition systems.

Algorithm 5.3: Definition of the pupil dilation limit algorithm.
Purpose: to determine the limit of pupil dilatation.
Input: Iris images.
Result: The pupil dilation limit.
Procedures:
Step 1: Assemble a set of iris image data that contains many irises for the same class that have significant variations in the dilatation degrees of the pupil.
Step 2: segment the irises in the selected data set and code each iris in it to create your iris code.
Step 3. Compare each diaphragm pattern in the data set with all other iris patterns in the data set.
(A) compare irises in the same class to generate an intra-class distribution of comparisons.
(B) compare the irises in different classes to generate a distribution of inter-class comparisons.
Step 4: Calculate FMR and FNMR for this dataset.
Step 5: Eliminate irises whose degree of dilation exceeds a certain limit X from the data set, where the first value of X is equal to the highest degree of pupil dilation in the data set.
Step 6: Gradually decrease the value of X and repeat steps 1 to 5.
Step 7: Get the limit value of X, which minimizes the number of errors.
Many previous studies have attempted to test the effect of pupil dilatation on the iris diaphragm pattern and show how different degrees of stretching affect the performance of the iris biometric system. But none of the previous works has calculated the extent of the pupil expansion, if the dilation exceeds it, this will affect the operation of the biometric system of the iris. In other words, the restriction of pupil growth, in which the pupil dilation in the iris should not exceed it, will be determined to achieve the best results. To find this limit, the following steps are proposed in Algorithm 5.3. The experimental results in Section 5.2 show that there is

a limit to slowing the pupil, which, when the degree of dilatation exceeds it, affects the operation of the iris recognition system.

5.4 Iris code bit analysis

Identification and verification of people using iris biometrics depends on many factors. Artifacts of contact lenses, hair occlusion, pupil dilatation, eyelids, eyelashes and specular highlights distort the appearance of the texture and increase the errors of FMR and FNMR. Recently, a new problem has been discovered that also affects the performance of the iris recognition system, these are uncoordinated bits or fragile bits. For a given iris, a little bit of its iris code will be called "fragile" or inconsistent if there is any significant probability that it will end with zero for some images of the iris, and one for the other images of them. These bits can significantly degrade the performance of the iris recognition. Therefore, the existence of unmatched bits in the data set will be investigated using the following steps in Algorithm 5.4

Algorithm 5.4: Analysis of the Iris code algorithm.

Purpose: analysis of iris code.
Input: Iris images.
Result: Proof that the iris code contains some inconsistent bits.
Procedures:
Step 1. The collection of iris image data has such a high detail texture.
Step 2: segment the irises in the selected data set and encode each iris in it to create your iris code.
Step 3: Compare the iris patterns for the same person to determine which bits are consistent or inconsistent. Let X be the percentage of bit retention (if X = 70% means that this bit remains zero or one in 70% of the iris images for the same person).
• If any bit retains its value by a percentage greater than X, it is marked as consistent.
• If any bit retains its value by a percentage less than X, it is marked as inconsistent.

The value of X can be chosen so that it corresponds to the capture device and the selected data set. After determining the consecutive and inconsistent bits in our data set, we can use the result in several ways. Here we use consecutive and inconsistent bits to examine the areas in which these bits exist. Algorithm 5.5 explains the steps of our method to determine which areas are more significant than others in the iris code.

Algorithm 5.5: Determining the best regions in iris code algorithm.

Purpose: To determine the best regions in the iris code.
Input: Iris images.
Result: Prove that the inner areas in the iris code are better than the outer areas in the iris code.
Procedures:
Step 1. Collection of iris image data with high texture detail.
Step 2: segment the irises in the selected data set and encode each iris in it to create your iris code.
Step 3: Divide the iris code into four parts, each part with 5x480 bits
Step 4: Mask each part separately and perform a matching test, the same as in Algorithm 5.2, and calculate the FNMR for each of them.
Step 5: Compare the results

Chapter 6 Results and Discussion

In this chapter, we describe the generally available and freely accessible iris image database that will be used in this thesis. Then, the selected and used data sets are displayed in the experiments. Finally, we show and discuss the results of our experiments.

6.1 Public Databases for Iris

For a fair comparison of recognition methods, similar initial data are required for comparison and evaluation of their results. Therefore, standard iris' databases assume high relevance and become indispensable in the development process. On the Internet, there are many iris image databases, such as CASIA, UBIRIS, MMU, ICE, WVU and UPOL. In this section, we describe the main characteristics of the generally available and freely available iris database for biometrics that will be used in experiments.

6.1.1 CASIA Database

The image database CASIA Iris (CASIA-Iris), developed by the Chinese Academy of Sciences Institute of Automation research group. This database was released to the international community of biometric systems and updated from CASIA-IrisV1 to CASIA-IrisV4 since 2002. More than 3,000 users from 70 countries or regions downloaded CASIA-Iris, and on the basis of this data, a great work was done to recognize the iris of the Iris eye.

Casia-IrisV1

The image database CASIA Iris Version 1.0 (or CASIA Iris-V1) is probably the first iris imaging database that is widely available to iris researchers and is widely used. It includes 756 images of the iris of 108 eyes, hence 108 classes. For each eye, 7 images are recorded in two sessions, where three samples are collected in the first and four in the second session. His images were captured in a medium with a high degree of confinement, which determined the characteristics of the images obtained. They represent

Very close and homogeneous characteristics, and their noise factors are exclusively associated with iris obstruction by eyelids and eyelashes.

Casia-IrisV2

The image database CASIA Iris Version 2.0 (CASIA-IrisV2) includes two subsets, assembled using two different devices: Irispass-h, developed by OKI, and a self-developed CASIA-IrisCamV2 device. Each subset includes 1200 images from 60 classes.

CASIA-IrisV3

CASIA-IrisV3 includes three subsets, which are designated as CASIA-IrisV3-Interval, CASIA-IrisV3-Lamp, CASIA-IrisV3-Twins. CASIA-IrisV3 contains a total of 22,035 images of the iris of more than 700 items. All images of the iris are 8-bit JPEG files with gray level, collected under near infrared illumination. Almost all Chinese subjects, with the exception of some in CASIA-IrisV3-Interval. Since the three sets of data were collected at different times, only CASIA-IrisV3-Interval and CASIA-IrisV3-Lamp have a small overlap in the subjects. This database is used by many researchers to investigate the effectiveness of their algorithms. CASIA-IrisV3 includes three subsets that are marked as

1. CASIA-IrisV3-Interval: Iris images were captured by very good image quality with extremely clear details of the iris texture.

2. CASIA-IrisV3-Lamp: Iris images have a non-linear deformation due to variations in visible illumination. The lamp turned on / off near to the object to make more intra-class changes when collecting this database. As a result of switching on / off the lamp near to the object, the pupil will dilate and contract, and irises will be generated with different degrees of dilatation of the pupil. CASIA-IrisV3-Lamp contains 16213 aperture images for 819 classes

3. CASIA-IrisV3-Twins: the first public iris image data set of twins.

CASIA-IrisV4

CASIA-IrisV4 is an extension of CASIA-IrisV3 and contains six subsets. Three subsets from CASIA-IrisV3 are CASIA-Iris-Interval, CASIA-Iris-Lamp and CASIA-Iris-Twins, respectively. Three new subsets: CASIA-Iris-Distance, CASIA-Iris-Thousand and CASIA-Iris-Syn. CASIA-IrisV4 contains a total of 54,601 images of the iris of more than 1,800 genuine subjects and 1,000 virtual subjects. All images of the iris are 8-bit JPEG files with gray level, collected under near infrared illumination or synthesized. Six sets of data were collected or synthesized at different times, and CASIA-Iris-Interval, CASIA-Iris-Lamp, CASIA-Iris-Distance, CASIA-Iris-Thousand

can have a small overlap between subsets in subjects. CASIA-Iris-Interval is selected for use in our analysis of the iris code, because the images of the iris are captured very clearly. CASIA-Iris-Interval is well suited for studying the detailed textural features of images of the iris.

6.1.2 UBIRIS Database

The main target of the UBIRIS database is to minimize the need for collaboration with users, that is, the analysis and suggestion of methods for automatic face recognition using images of their iris taken at a distance and minimizing the required degree of cooperation from users, possibly even in convert mode. The UBIRIS database has two different versions:

UBIRIS.v1

- This version of the database consists of 1877 images collected from 241 eyes during September 2004 in two separate sessions. It imitates less limited visualization conditions. The images in this database were saved in TIFF format in the RGB color representation. The Nikon E5700 camera was used to capture this database, and this is the first diaphragm database taken at visible wavelength. It's public and free.

UBIRIS.v2

- The second version of the UBIRIS database contains more than 11,000 images (and is constantly growing) and more realistic noise factors. The images were actually captured at a distance and in motion.

6.2. The results of the proposed segmentation algorithm

In the proposed segmentation algorithm, we begin the implementation with clustering of K-means, followed by edge detection and circular Hough transformation, as shown in Figure 4.1. We assume that both the iris and the pupil have a circular shape. So, each circle is completely described by the values of its center (x, y) and its radius r. We believe that segmentation is accurate when two circles of the iris and the pupil fall precisely into the iris and the pupil of the borders.
After applying the proposed iris segmentation algorithm to UBIRIS v1 (Session 1), we get segmented images, as shown in Figure 6.1. After that, we calculate the

accuracy (the segmentation is accurate when two circles of the iris and the pupil fall exactly within the boundaries of the iris and the pupil) of the images obtained.

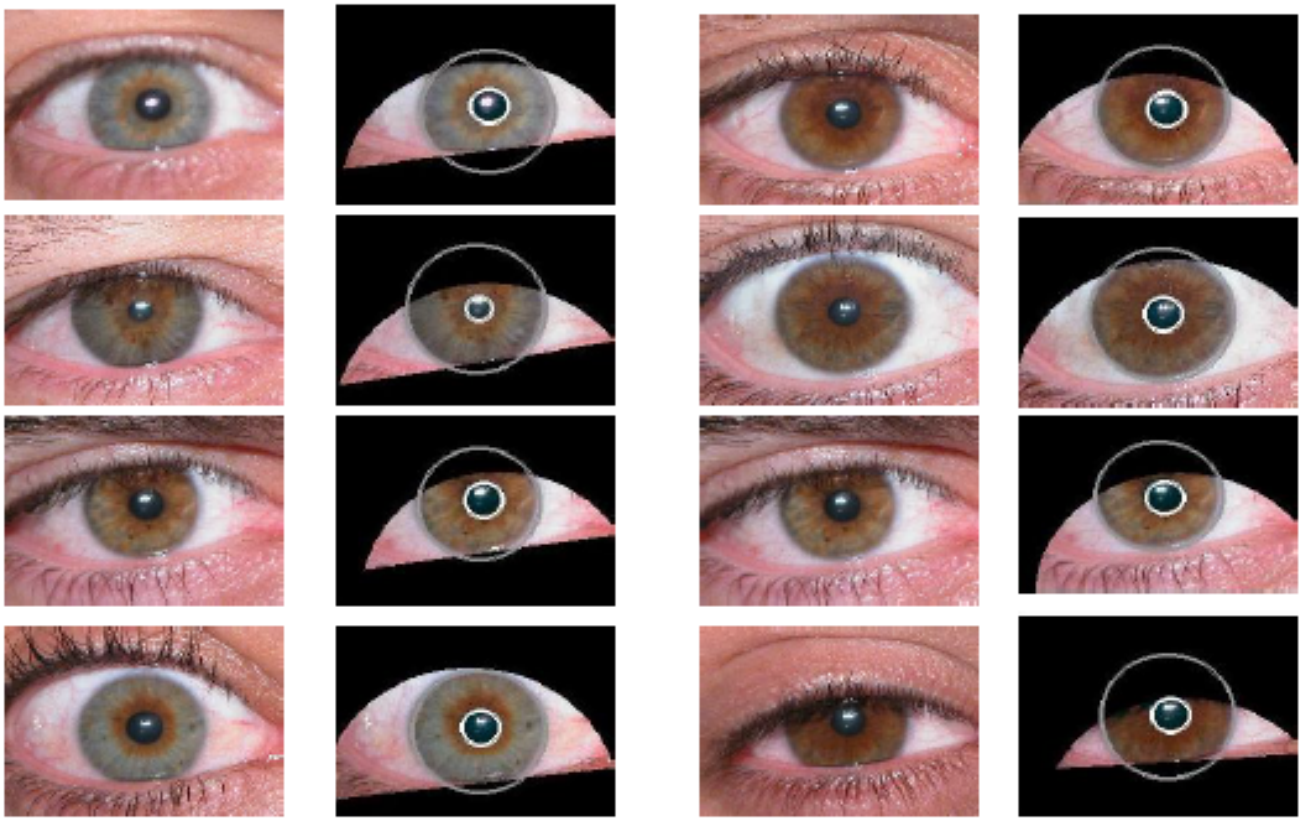

Figure 6.1: Examples of correct segmented irises.

Table 6.1 compares the accuracy of previous segmentation algorithms (experiments performed approximately in the same hardware environments) described in Sections 2.1.

Table 6.1: Comparison between the accuracy of proposed algorithm with some previous algorithms.

Method	Accuracy	Time (s)
Daugman	95.22%	2.73
Camus and Wildes	98.68%	1.95
Martin-Roche	77.18%	2.91
Proposed	98.76%	1.49

As the results show, the proposed accuracy of the algorithm is better than the algorithms of Daugman and Wiles. At the same time, the execution time of our segmentation algorithm is the lowest, because the various proposed steps that are used to reduce the search areas in the circular transformation of Hough. The proposed algorithm failed to segment noisy irises, when eyelids and eyelashes cover large parts of the iris (more than 60%) or when the upper or lower eyelid closes the iris pupil (note that most segmentation methods do not work in these cases). In Fig. 5.2 shows examples of failed images of iris segmentation.

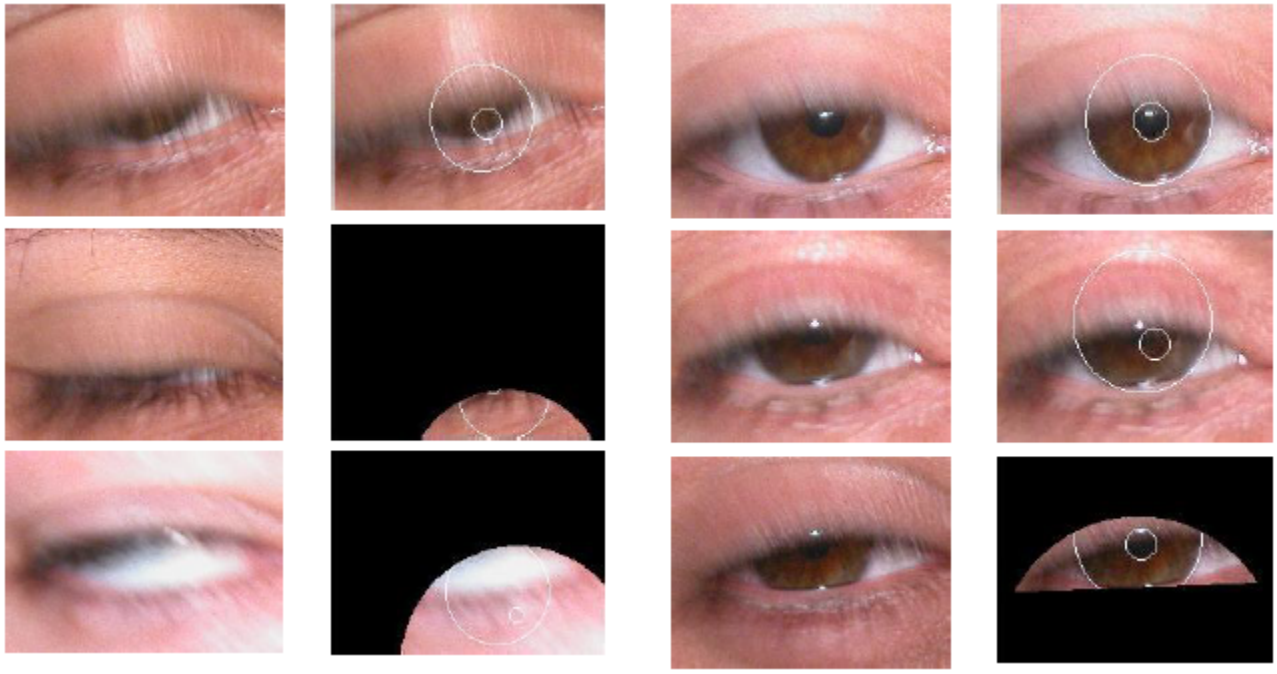

Figure 6.2: Examples of unsuccessful segmented noisy irises, when eyelids and eyelashes cover large parts of the iris.

In the second column of Fig. 6.2 our segmentation algorithm failed because the iris is approximately completely covered by eyelids. In the fourth column, the segmentation algorithm successfully localizes the iris border, but when the pupil's border is localized, when it is covered by eyelids, the pupillary boundary cannot be localized, and the eyelid region cannot be isolated when the iris image is blurred due to rapid movements during image capture.

To assess the effectiveness of the proposed segmentation method throughout the recognition system, we implement the other three steps (normalization, coding, comparison). Some functions of the Masek iris recognition algorithm are used. The implemented system is used to generate an iris pattern code for each iris. To draw a

match and non-match the distributions for this database, each image of the iris in the database
Compared with other irises in the database. For the Iris UBIRIS v11 database session, the total number of comparisons is 1 448 410, where the total number of intra-class comparisons is 2410, and the total number of comparisons between classes is 1 446 000. In the comparison stage, HD is used as a measure of the dissimilarity between the two IRIS' codes codeA and CodeB:

$$\frac{||(\boldsymbol{codeA} \otimes \boldsymbol{codeB}) \cap \boldsymbol{maskA} \cap \boldsymbol{maskB}||}{||\boldsymbol{maskA} \cap \boldsymbol{maskB}||}$$

Where maskA and maskB are masks of code A and codeB, respectively. The mask proposed by Daugmann means that the area of the iris is closed by eyelids, eyelashes, brightness, therefore it reflects the results achieved. Therefore, HD is a fractional measure of dissimilarity after the noise regions are discounted.
Figure 6.3 shows the Hamming distance distribution using our segmentation algorithm. Figure 5.4 shows the Hamming distance distribution using the Daugman segmentation algorithm. The results show that the distribution of matches when using our algorithm shifted a significant distance to the left. The average value of the match distribution decreased by 0.12. In Figure 6.4, the distance between the two means is 0.075, and the distance between the two means in Figure 6.3 is 0.19. We notice that the distance between the match and the non-match distribution increases because the proposed segmentation algorithm is used, as a result, the error rate will be reduced and a significant improvement will be achieved compared to the performance of the Daugman algorithm.

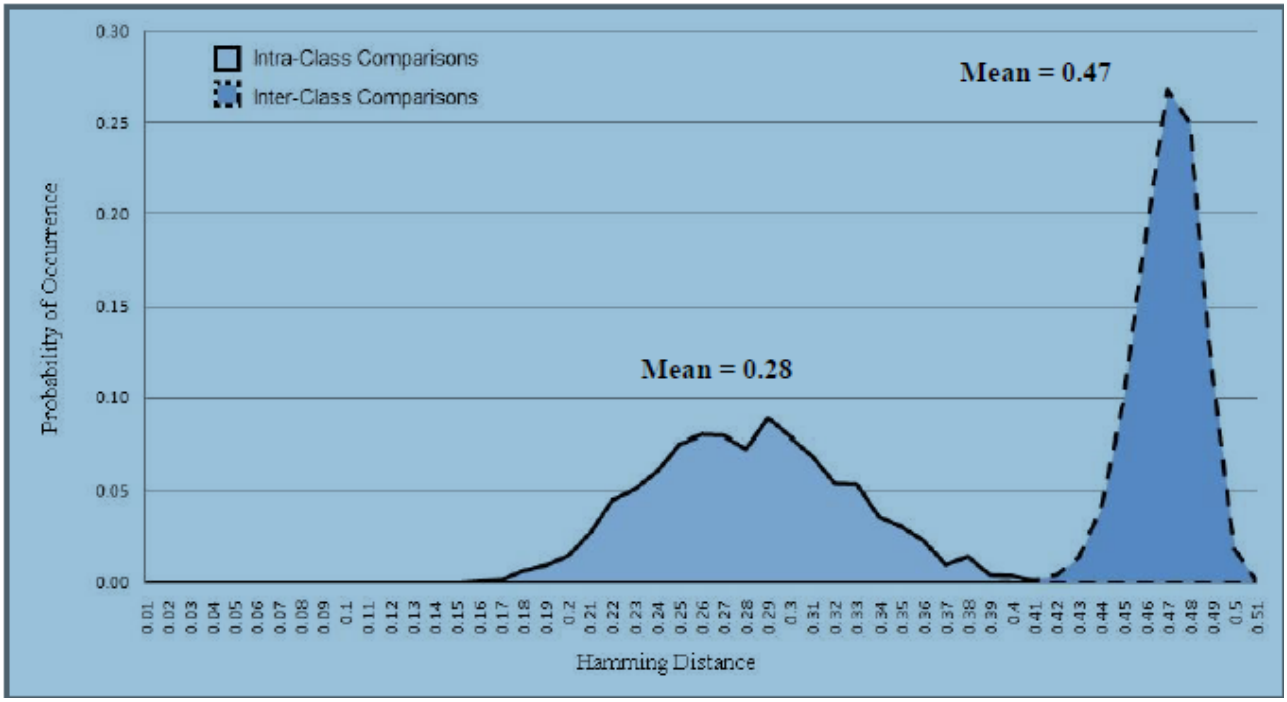

Figure 6.3: The match and non-match distributions for UBIRIS v1 when our segmentation algorithm is used.

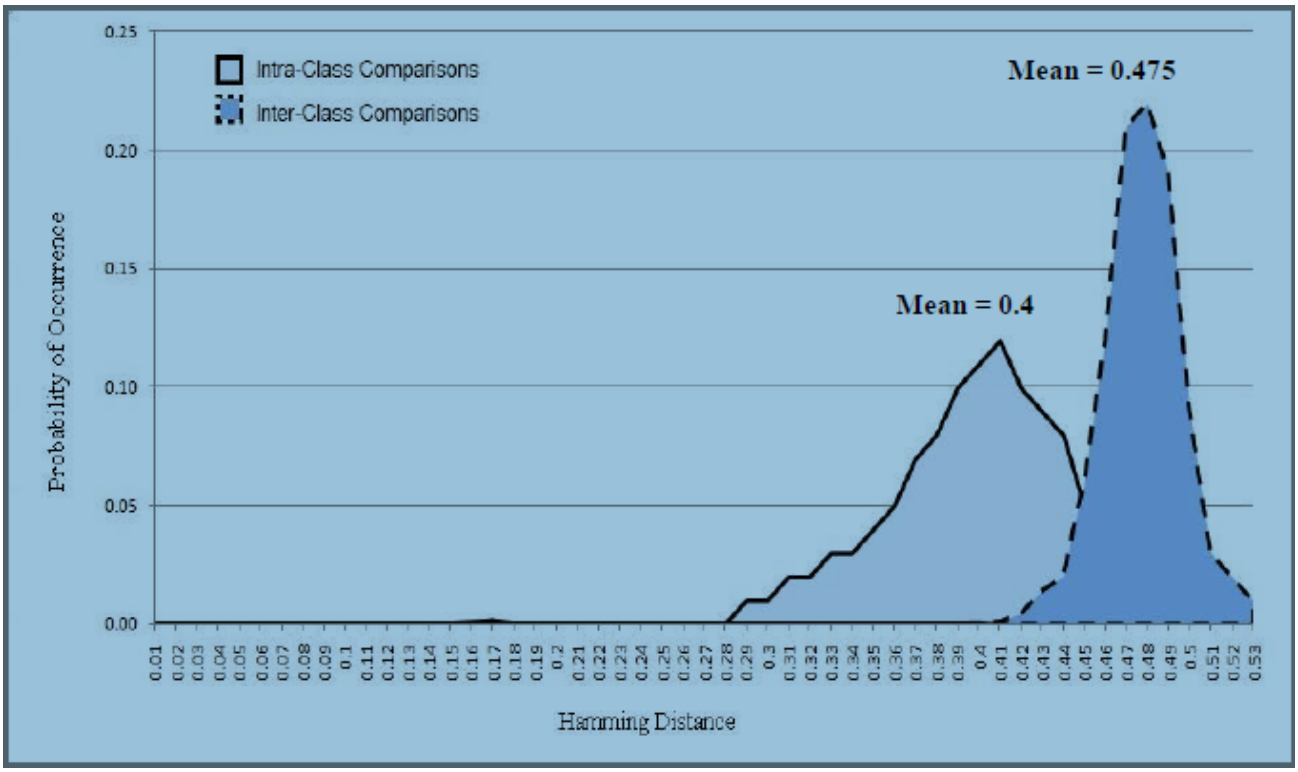

Figure 6.4: The match and non-match distributions for UBIRIS v1 when Daugman algorithm is used.

In addition, it is noted that when using the proposed segmentation algorithm, the interference of the coincidence and discrepancy distribution is less than when using the Daugman segmentation algorithm. This is due to the fact that Daugman's segmentation algorithm is very sensitive to noise and cannot cope with noise factors that arise in non-ideal conditions, such as mirror reflections, pupil isolation and eyelid occlusion. Figure 6.5 shows the EER of the iris recognition system when our proposed algorithm is used. In EER point FMR and FNMR are almost equal. EER allows you to evaluate FMR and FNMR in one operating point. EER is very low when the proposed segmentation algorithm is used compared to the EER of the iris recognition system when the Daugman segmentation algorithm is used. This result shows that the proposed segmentation algorithm accurately isolates the error regions in the iris template. Thus, FMR and FNMR will decrease. Daugman's segmentation algorithm could not handle with these sources of errors, since it is designed to work in ideal conditions and uses the operator Integrodifferential, which often fails when the images do not have sufficient separation between the iris and sclera.

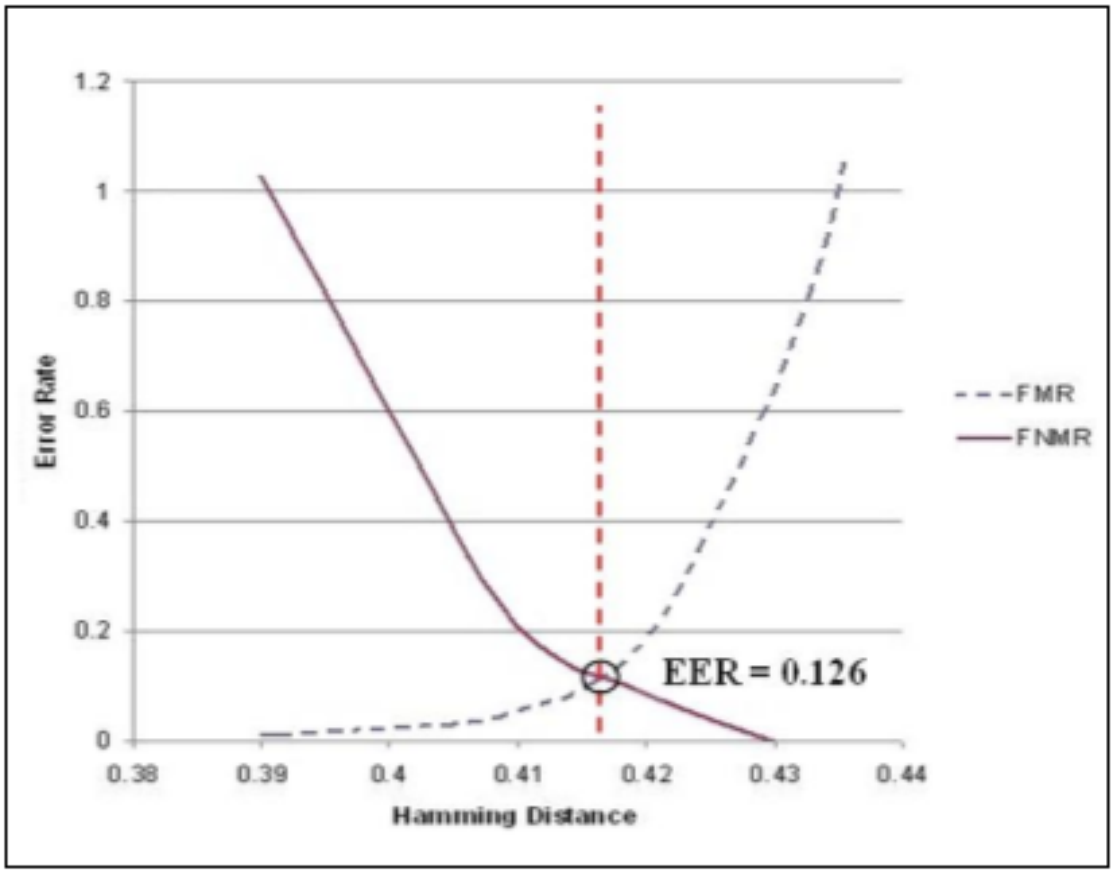

Figure 6.5: The Equal Error Rate value where FMR and FNMR are equal.

To assess the effectiveness of the proposed segmentation algorithm using various techniques, the Daugman method is realized using some functions from the Masec iris recognition algorithm and the results described in. We select the most important points to compare our algorithm with other, which is FAR (%) at 0.0001% FRR and FRR (%) at 0.0001% FAR. The experimental results for the three algorithms are summarized in Table 6.2. This table shows that the proposed segmentation algorithm significantly reduces two metric values. As we have already said, the good results of our segmentation algorithm are due to its ability to handle any source of error type that can occur in non-ideal environments.

Table 6.2. Comparison of the algorithm with the previous two algorithms.

Method	**FAR(%) at 0.0001% FRR**	**FRR(%) at 0.0001% FAR**
Daugman	7.2	12.96
SVM Match Score Fusion	5.9	8.71
Proposed	1.5	5.82

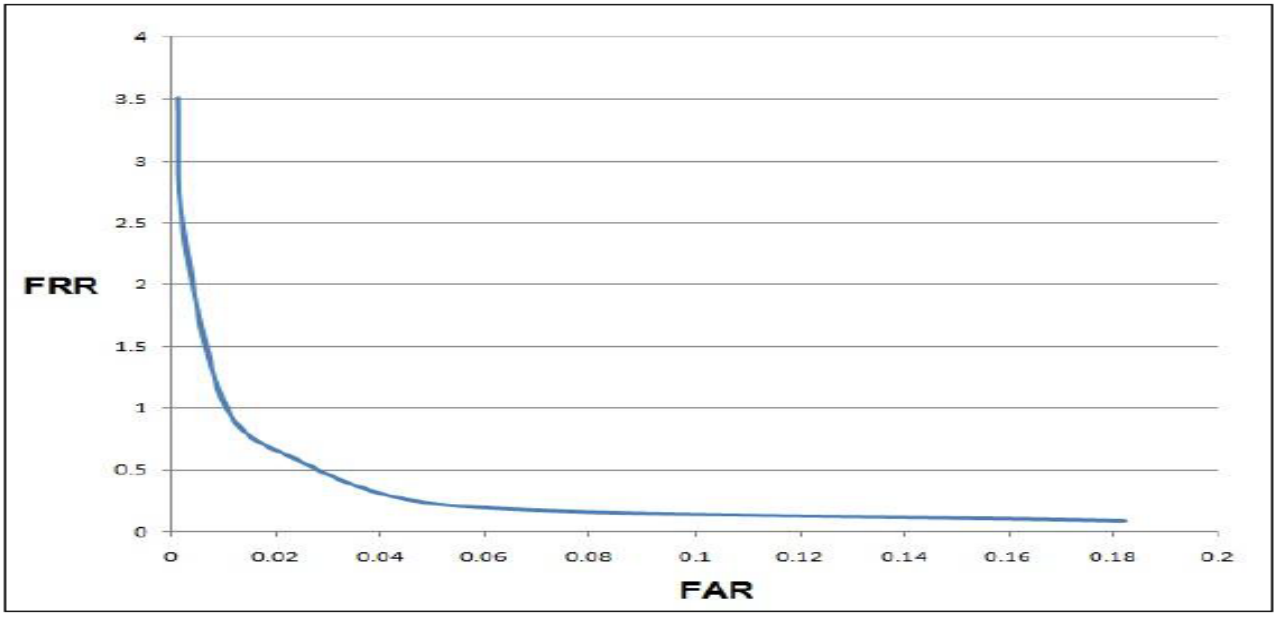

Figure 6.6: ROC curve, reflecting the relation between the FAR and FRR.

Figure 6.6 shows the ROC curve when proposed segmentation algorithm is used. From this figure, it can be seen that FAR and FRR are approximately equal to 0.16, which is a very low value. Contrariwise, FRR increases faster than FAR, it does not affect the iris recognition system very much, because the most important safety value is FAR. As mentioned in Section 2.4, FRR and FAR can be adjusted to reflect their respective costs and benefits. It depends on the application that will be used by the iris recognition system.

6.3 Results of Pupil Dilation

6.3.1 Dataset

In experiments on the dilatation of the pupil, we use CASIA-IrisV3, as described in Section 6.1. We did not use whole images of this database, because many images of irises do not greatly affect the on / off of the lamp close to the object. As a result, many images have approximately the same level of pupil dilatation for the same class, which will not help in our research. Therefore, 721 images for 41 people are selected from the CASIA-IrisV3-Lamp database. The selected data set contains the best images in the database, which have a high variation in the degrees of pupil dilation for the same class, and at the same time the iris is not affected by different types of noise (poor focusing, Iris obstructions due to eyelashes, motion blurred, iris obstructions due to eyelids, iris with specular reflections ...). Thus, only one type of noise affects the selected data set, which is the difference in the degrees of pupil dilatation. In Fig. 6.7 shows the high variation in pupil dilation degree of the three classes from the selected data set. The degree of pupil dilation is calculated by obtaining the radius of the pupil and the radius of the iris. So, first, we need to localize and segment each iris in our data set, then we get the radius of the iris and the pupil. All the irises of the data set are truly segmented because they are chosen carefully, and if any iris has an inaccuracy in its segmentation, we exclude it from the data set in the selection step, as was said earlier, to make our data set with only one problem or source of error. This is the dilatation of the pupil.

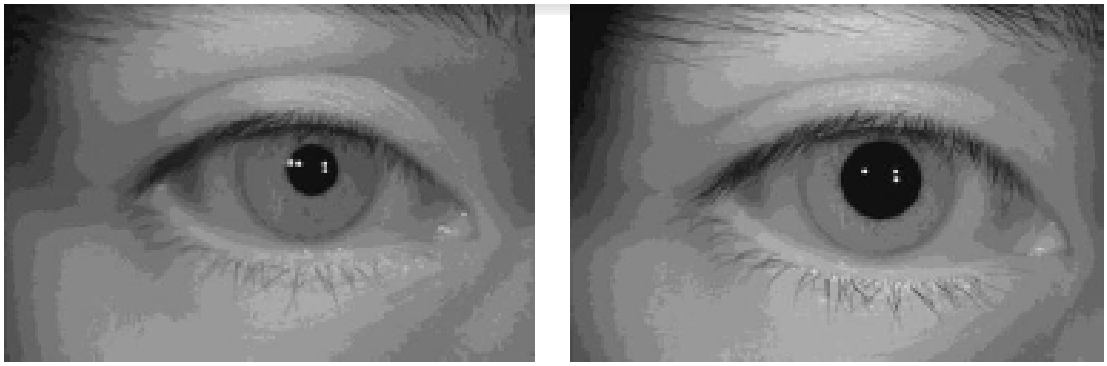

Figure 6.7: The big difference of pupil size in our selected dataset.

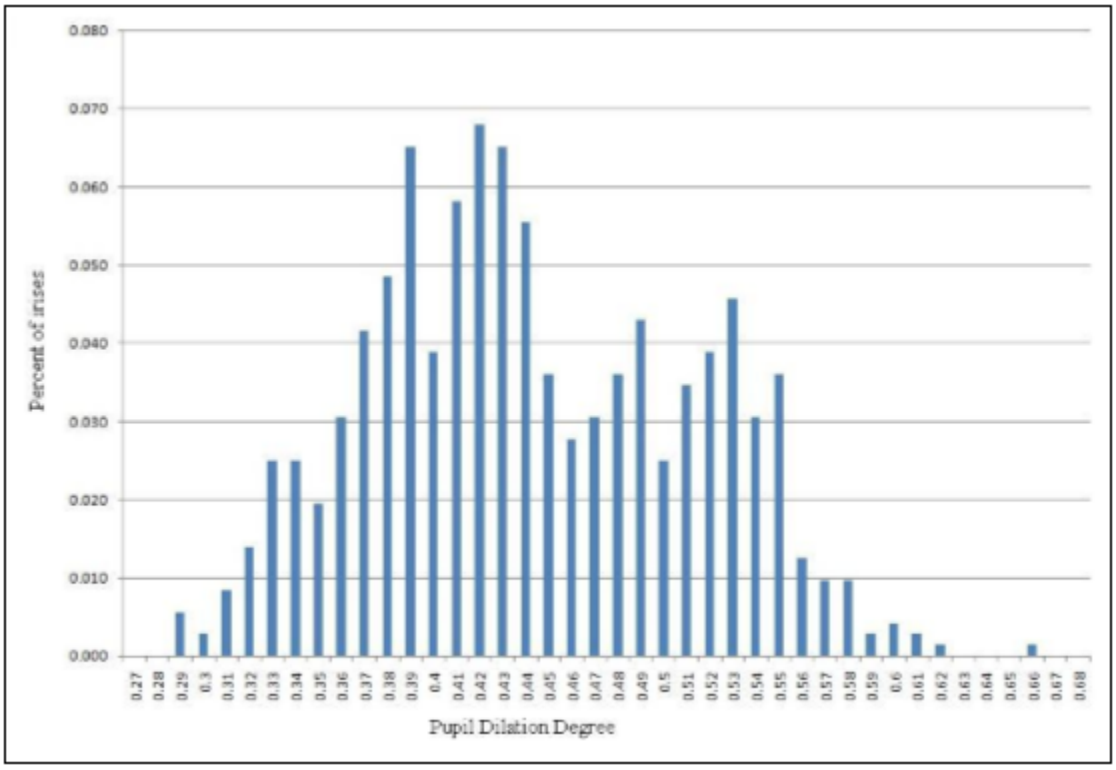

Figure 6.8: Pupil dilation ratios in our dataset.

To measure dilation, we use a simple method which used by many researchers. This process measures the degree of dilation by dividing the radius of the pupil by the radius of the iris. Since the radius of the pupil is always less than the radius of the iris, this ratio of dilation should be between 0 and 1. In the selected 721 images, all dilation ratio was from 0.28 to 0.66. The distribution of the dilation ratio is shown in Figure 6.8. It is noted that the data sets have wide differences in the pupil dilatation degree, which will be needed when evaluating the dilatation effect in good and fair experiments.

6.3.2. Impact of pupil dilation on performance

To show that the pupil dilation affects the operation of the iris recognition system, all the irises in our data set are first segmented using a circular Hough transform to detect the boundaries of the iris and pupil. This is due to the first use of the Canny edge detection to create an edge map. The gradients were shifted in the vertical direction for the outer border of the iris / sclera, as suggested by Wilde. In cases where the segmentation software detects occlusion by eyelid, parts of the iris region are masked (Figure 6.9). This can restrict the effect of eyelids and eyelashes on the results.

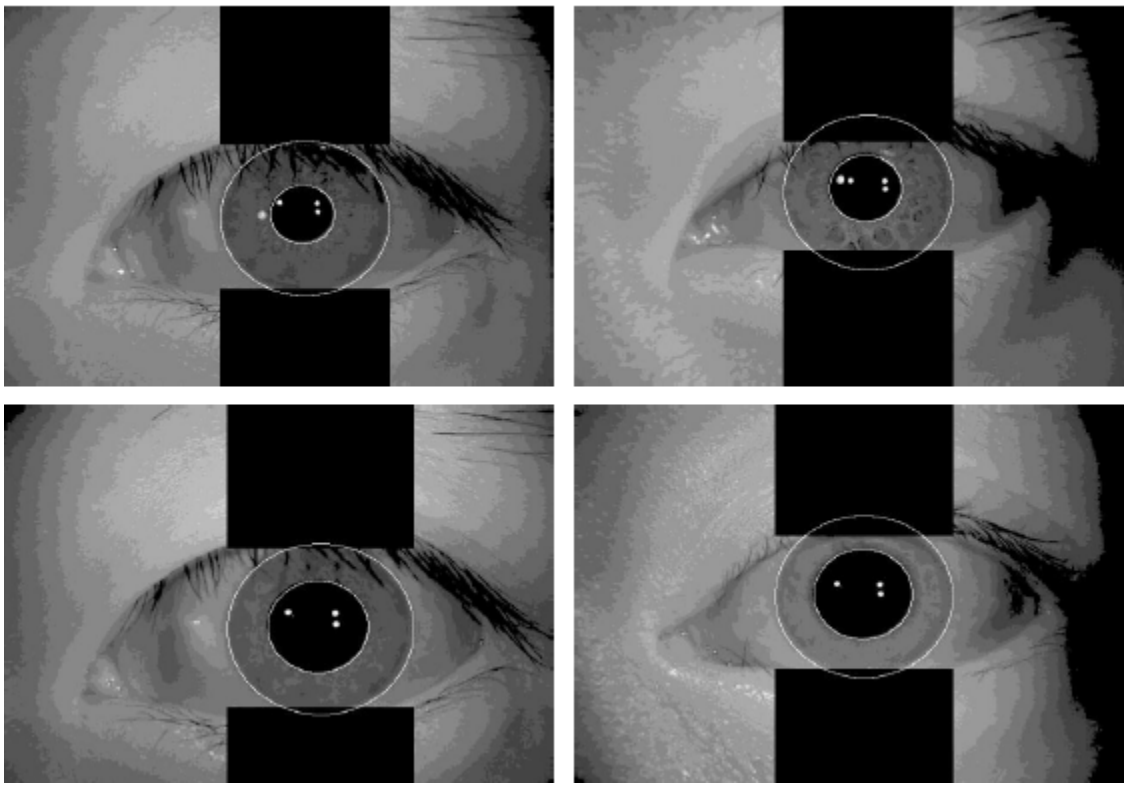

Figure 6.9: Samples of noise irises from selected dataset that segmented and masked.

After that, the segmented irises are normalized using the Daugman approach. At the function encoding stage, we reduce the normalized iris diagrams using 1D Log-Gabor wavelets to create a 2x20x240 bit iris pattern for each iris. The MATLAB-code Masek is used. We divide the irises into two groups: irises with a dilatation degree of the pupil less than 0.5 and irises with degrees of dilatation of the pupil greater than or equal to 0.5. Then we compare each iris pattern in the data set with the other iris patterns in two cases. When using all images and excluding irises in the second group (the degree of dilatation is more than 0.5). In the first experiment, the iris images

compared were 721. The total number of comparisons is 259,731, where the total number of infraclass comparisons is 6270, and the number of interclass comparisons is 253,461. At the comparison stage, we use HD as a metric of dissimilarity between the two iris codes considered. In the second experiment, the iris images compared are 555, after excluding 166 images in which the degree of pupil dilatation is greater than 0.5. Table 6.3 shows the result of each experiment. It is quite obvious that when irises with a high degree of pupil are excluded from the data set, FMR and FNMR decrease and the percentage of true compliance and true inconsistency increases. This means that irises with high degrees of pupil dilation cause more errors in the iris patterns. In Fig. 6.10 and Fig. 6.11 shows the match and non-match distributions for the first and second experiments, respectively.

Table 6.3: Comparison of results when using all irises and using irises with a degree of pupil dilution of less than 0.5.

Performance value	All irises in our dataset	Irises with pupil dilation degree less than 0.5
False Match Rate	0.027%	0.004%
False Non Match Rate	1.39%	0.69%
True Match Rate	99.973%	99.996%
True Non Match Rate	98.61%	99.31%

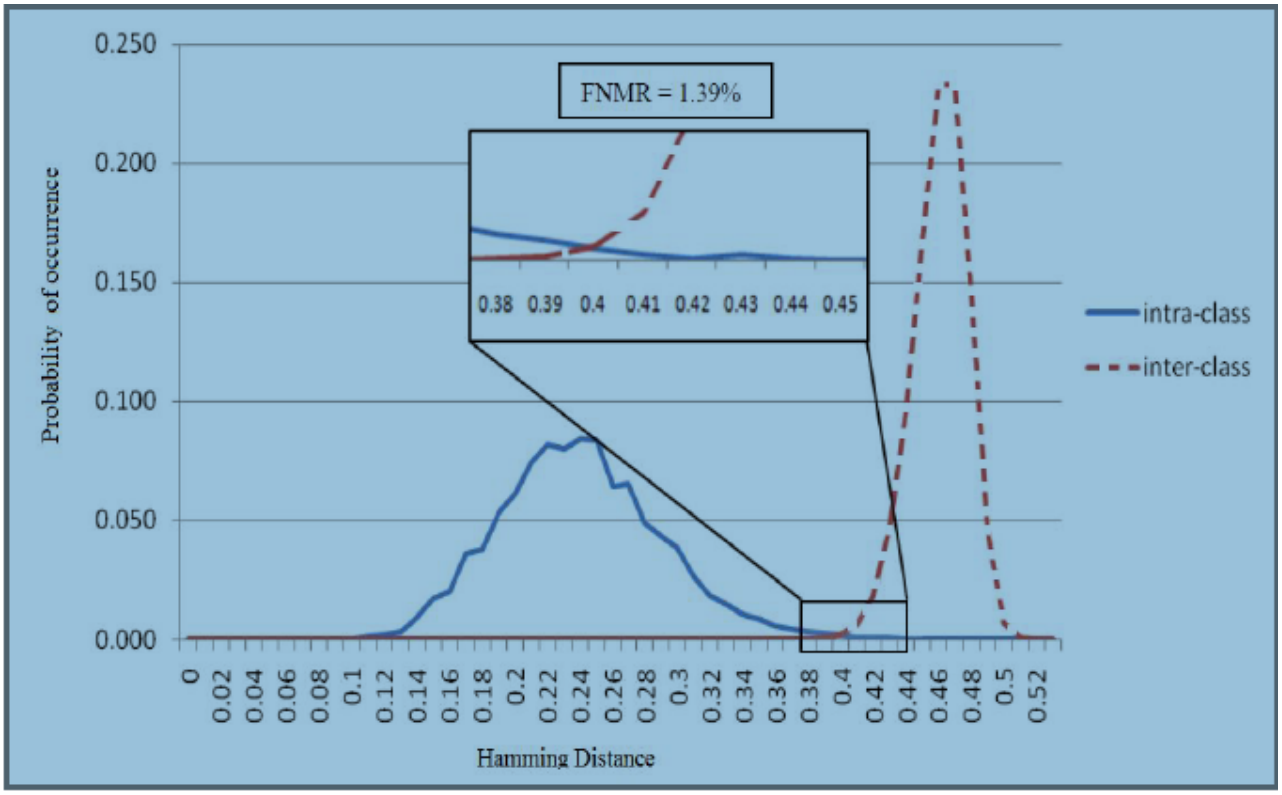

Figure 6.10: The match and non-match distributions for our selected dataset when all images are used.

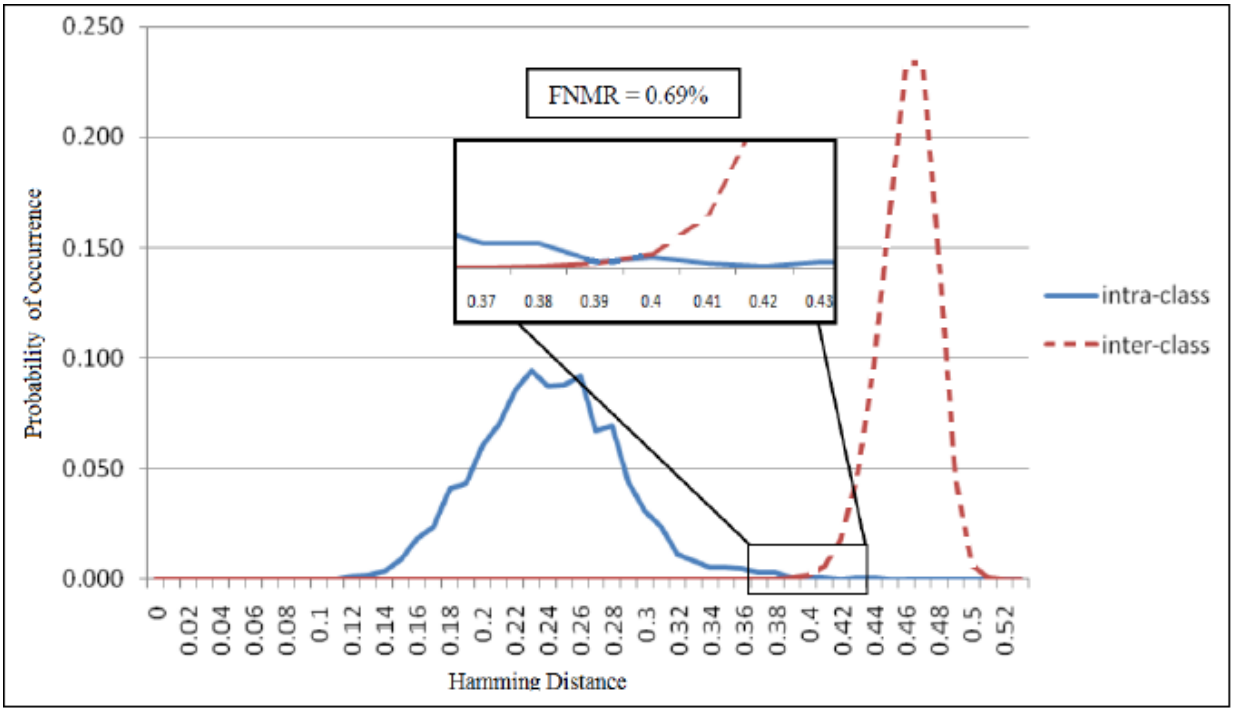

Figure 6.11. The distribution of match and nonmatch for the selected data set when images with a pupil dilution level of <= 0.5 are used.

As can be seen from the previous two figures, the FNMR decreases when we use the non-dilated pupil from 1.39% to 0.69%. At the same time, the true matching rate increases to 99.996%, which is a very good indicator. This means that the dilation of the pupil affects the identification and recognition processes, degrading some iris bits' in the iris' code. This error is caused by the assumption that when the pupil dilates, the stretching of the iris tissue in the radial direction is linear in the normalization process. Thus, the normalization of the iris causes some errors when comparing two images of different sizes, if the stretching of the iris is not linear. It is noticed that all irises stretch in a linear direction when the pupil is dilated, and also not all irises have non-linear stretching, when their pupil dilated. The behavior of dilation depends on many factors, such as eye color, eye health and human age. Therefore, we could not accurately predict the deformation of the iris, when the pupil dilates. Some researchers are trying to improve the efficiency of the recognition system in cases where the irises with dilated pupils are used to assess the parameters of the relative deformation between a pair of images or the modeling of nonlinear stretching of the iris as the sum of linear stretching and the Gaussian-deviation term. But, as we explained earlier, these algorithms do not completely solve the problem. Our idea is to prevent the spread of a large pupil (which causes errors in the iris code) from capturing images of the iris in the iris recognition system, rather than trying to cope with it. In other words, the important question to be asked is: What is the maximum degree of pupil dilatation that can be accepted by the recognition system while maintaining high accuracy in its work? The next section tries to answer this question.

6.3.3 The Pupil Dilation Limit

Many researchers try to test the effect of pupil dilatation on the iris pattern and examine how different degrees of dilatation of the pupil affect the performance of the iris biometric system. No preliminary work has been quantified: what is the degree of pupil dilatation, if the dilatation exceeds it, the performance of the iris biometric system will be affected. In other words, we will find a restriction on the pupil dilation that the pupil dilation in the iris should not exceed it to get the best results. In the next experiment, irises with a high degree of pupil dilation will be gradually eliminated from the selected dataset, and in each case all irises in the dataset will be segmented using the Hough circular transformation and edge detection. Then we mask the noise areas (for example, eyelashes, eyelids and reflections) with masks (see Figure 5.9). After that, we normalize and encode all irises to create a 2x20x480 bit iris template using the same methods used in section 5.3.2 for each iris. After generating all the patterns of all the irises, we compare each iris pattern in the database with all other iris patterns in the database, using the Hamming distance as the metric of the

differences between the two considered iris codes to obtain matches and nonmatches for the selected data set, when images with a dilation degree of the pupil <= Pdeg. Where P_{deg} is the degree of the pupil dilation, which irises with pupil dilation degree more than it, will be excluded from the dataset. P_{deg} will start at 0.66 (high dilation value of the pupil) and gradually decrease (0.61, 0.59, 0.58 ...). This means that at each stage the most dilated pupils are excluded from the data set, and then we calculate the FNMR error to estimate the effect of the excluded irises on the data set. Figure 6.12 shows the result.

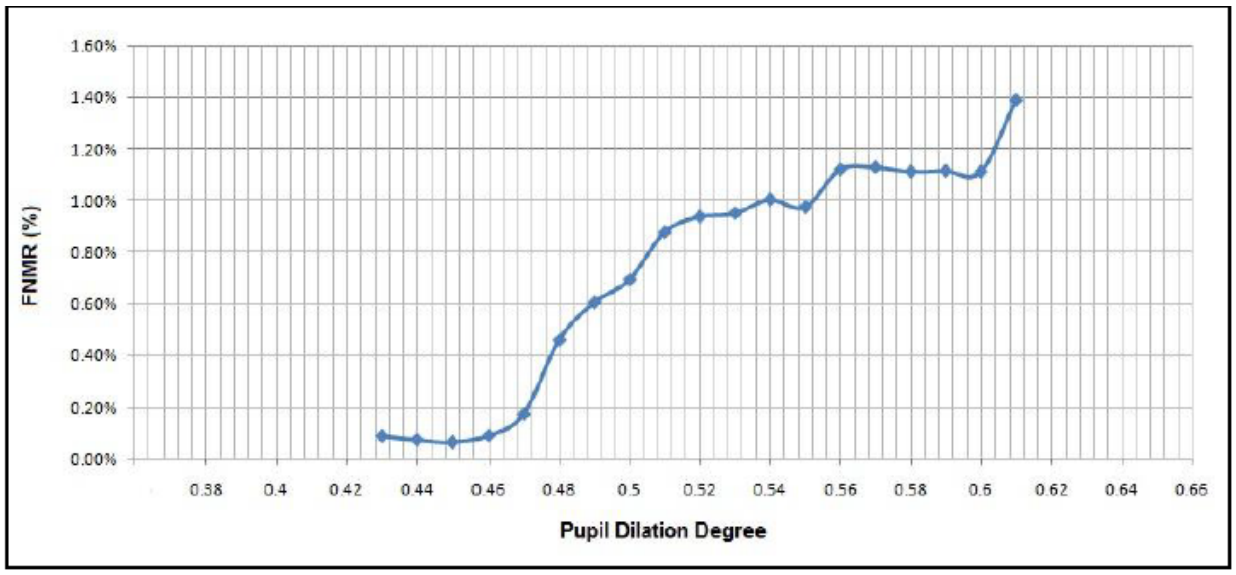

Figure 6.12: The FNMR when gradually remove irises with high pupil dilation degree.

As shown in Figure 5.12, minima on the graph appear when the degree of pupil dilation is 0.45, then the FNMR is 0.07%, and TNMR = 99.93%. Before and after 0.45, FNMR increases. The most important is the FNMR, when all the images in a data set are used in analysis without excluding any extended pupil template. We notice that the error value decreases, because we exclude the more dilated pupil templates from the data set, until we reach the degree of pupil dilation of 0.45. When we start excluding templates with a pupil dilation of 0.44 and 0.43, the FNMR starts to increase again. We notice that if you exclude this group of templates, the error staysthe same as it is, but the true matching rate decreases. It means that pupil dilation is not reason to the remaining error. As a result, we recommend obtaining a strong iris recognition system, the degree of expansion for any pupil should be less than 0.45. If the degree of the pupil dilation is greater than 0.45, we can use one of the previous proposed algorithms for the treatment of the pupil dilation. In Fig. 5.13 shows the match and nonmatch of distributions of our selected data set when images

with a pupil dilatation ratio <= 0.45 are used. Note that the FNMR error is reduced to 0.07.

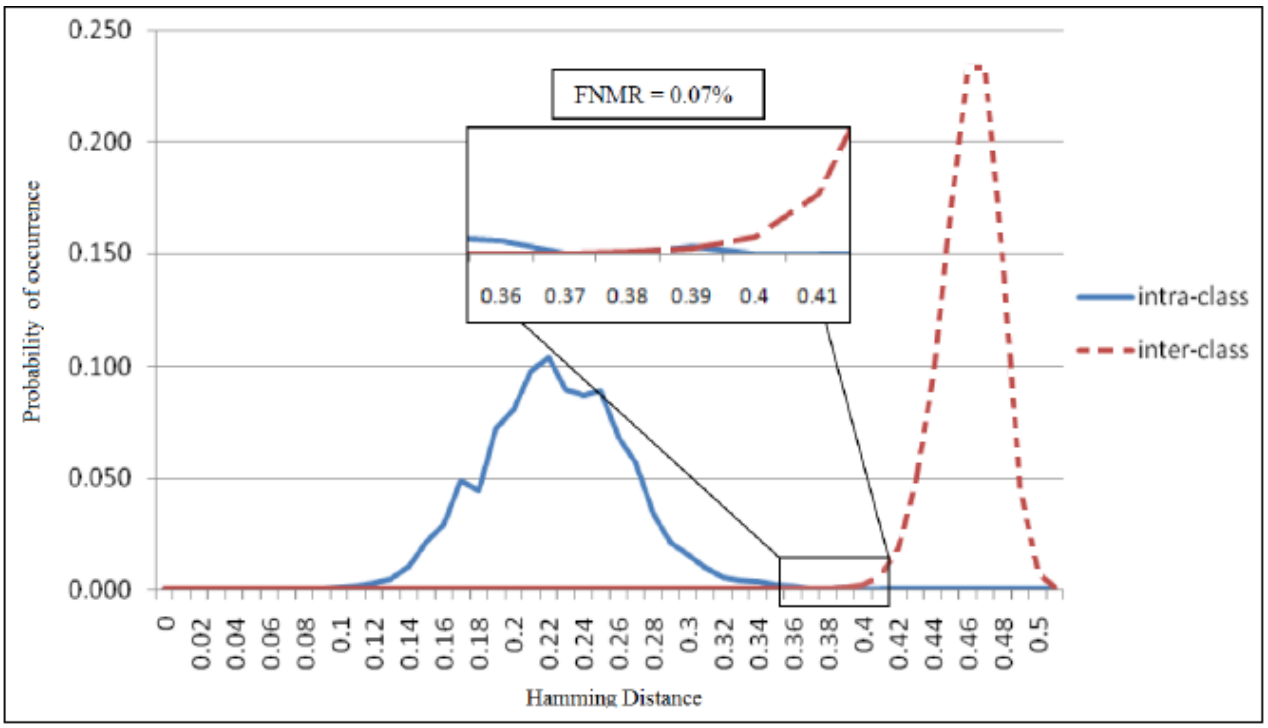

Figure 6.13. Comparison of match and non-match for your selected data set when images with pupil dilation degree <= 0.45 are used.

6.4 Analyzing Iris Code Bits

6.4.1 Dataset

CASIA-Iris-Interval was selected for use in this experiment. To study inconsistent bits in irises, we select 310 images from 22 people (160 images for the left eye and 150 images for the right eye). The best images from the CASIA-Iris-Interval database with high texture detail are selected, and the iris area does not affect different types of noise (poor focusing, motion blur, Iris gaps due to eyelashes, Iris obstacles due to eyelids, iris with specular reflections ...). All the irises in the data set are segmented to find the correct inner and outer boundaries of the iris using the circular Hough transform, and then the noise areas are masked when the segmentation software detects an occlusion caused by eyelids to minimize the effects of segmentation errors. Then all segmented irises are normalized and coded to create a 2x20x240 iris pattern for each iris using 1D log-gabor-bursts. In Fig. 6.14 shows the samples of the segmented irises of our selected data set from the CASIA-Iris-Interval database.

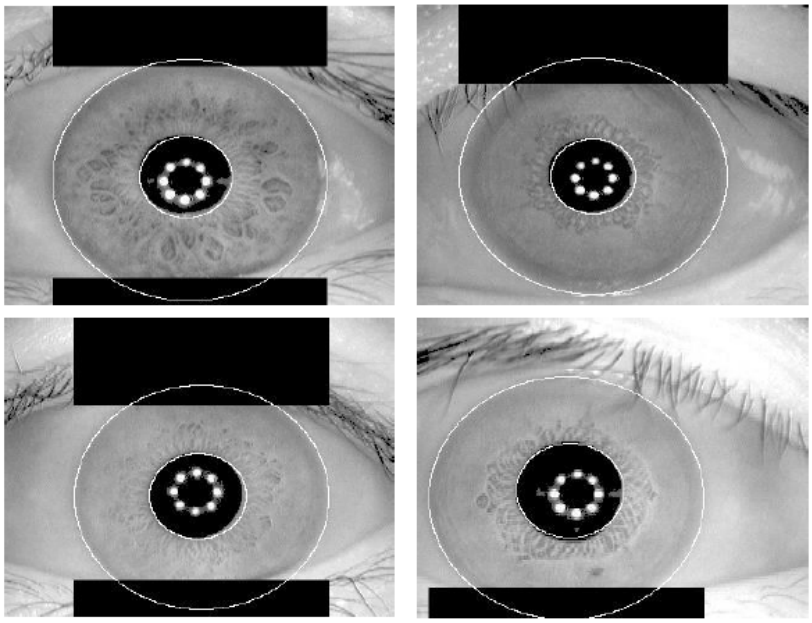

Figure 6.14: Samples of segmented irises from our selected dataset from CASIA-Iris-Interval database.

Each iris pattern is compared to all other iris patterns in the dataset, using the Hamming distance as the metric of the differences between the two iris codes examined. We mask all the noise and carefully select images of the iris. Errors FMR and FNMR are very small. This is important to focus analysis on fragile bits. The result is shown in Table 6.4.

Table 6.4: Error Rates of our selected dataset from CASIA-Iris-Interval.

Type	Rate
False Non Match Rate (FNMR)	0.212%
True Non Match Rate (TNMR)	99.788%
False Match Rate (FMR)	0.020%
True Match Rate (TMR)	99.980%

6.4.2 Inconsistent Bits

To examine the existence of unmatched bits in our selected data set, we create templates and masks for each iris, as shown in Figure 5.15. The real part and the imaginary part of these patterns are quantized to 0/1, giving two bits of the iris code for each result of the texture filter. Thus, the system used here generates an iris code of 2 x 20 x 240 = 9600 bits, and the mask of this code is 20x240 bits. To determine which bit is consistent (save its bit value to more than 80% of the images) or inconsistent (its bit value has changed by more than 20% of the images), the patterns and masks of irises of the same person are compared. The result of comparing templates and masks for three people is shown in Figure 5.16. For a more detailed view of the results, the real part (20x240 bits) and the imaginary part (20x240 bits) are separated. While the black bits represent unmatched bits, the white bits represent the matched bits. Below are two black rectangles - the area with a mask. We notice that the inner parts of the iris code are more consistent and better than the outer parts.

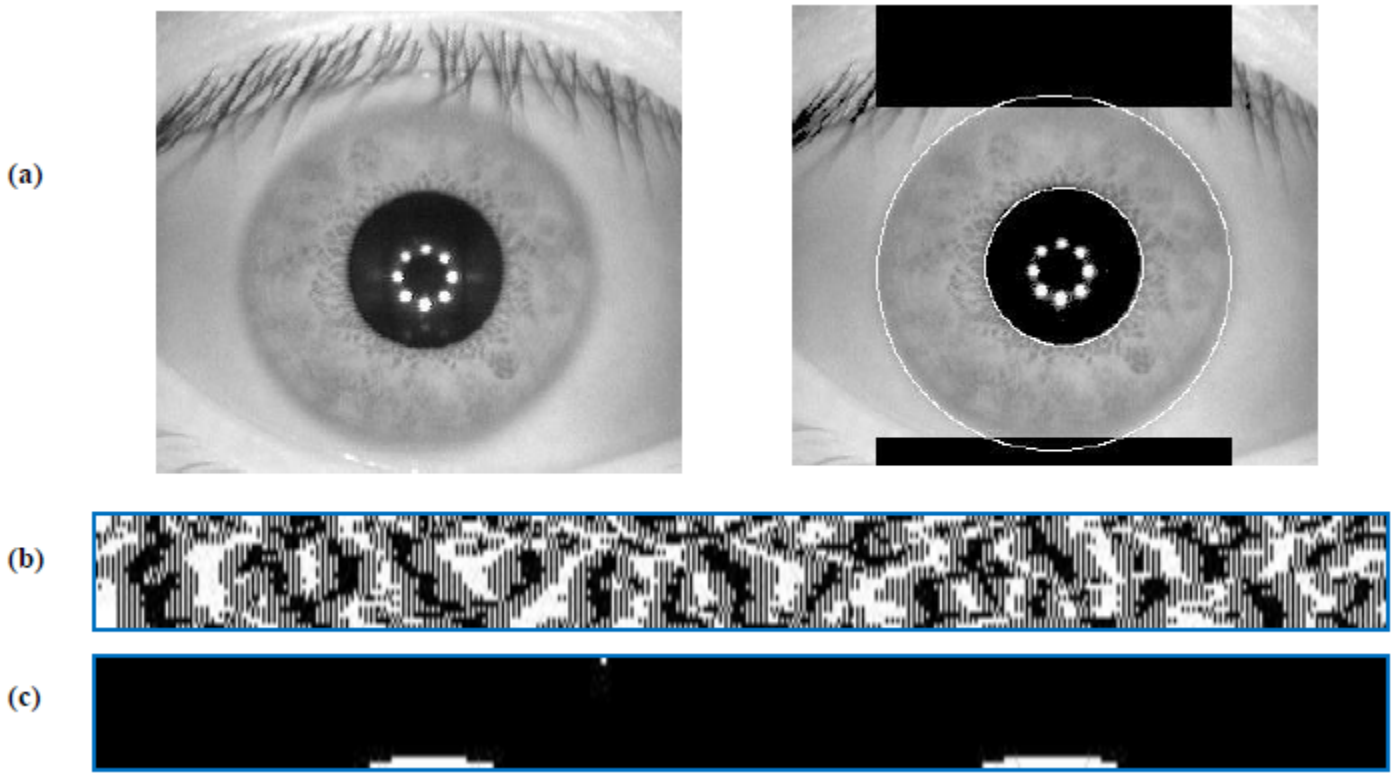

Figure 6.15: Sample of segmented and encoded iris from our selected dataset from CASIA-Iris-Interval database.(a) iris image before and after the segmentation. (b) iris template. (c) iris mask.

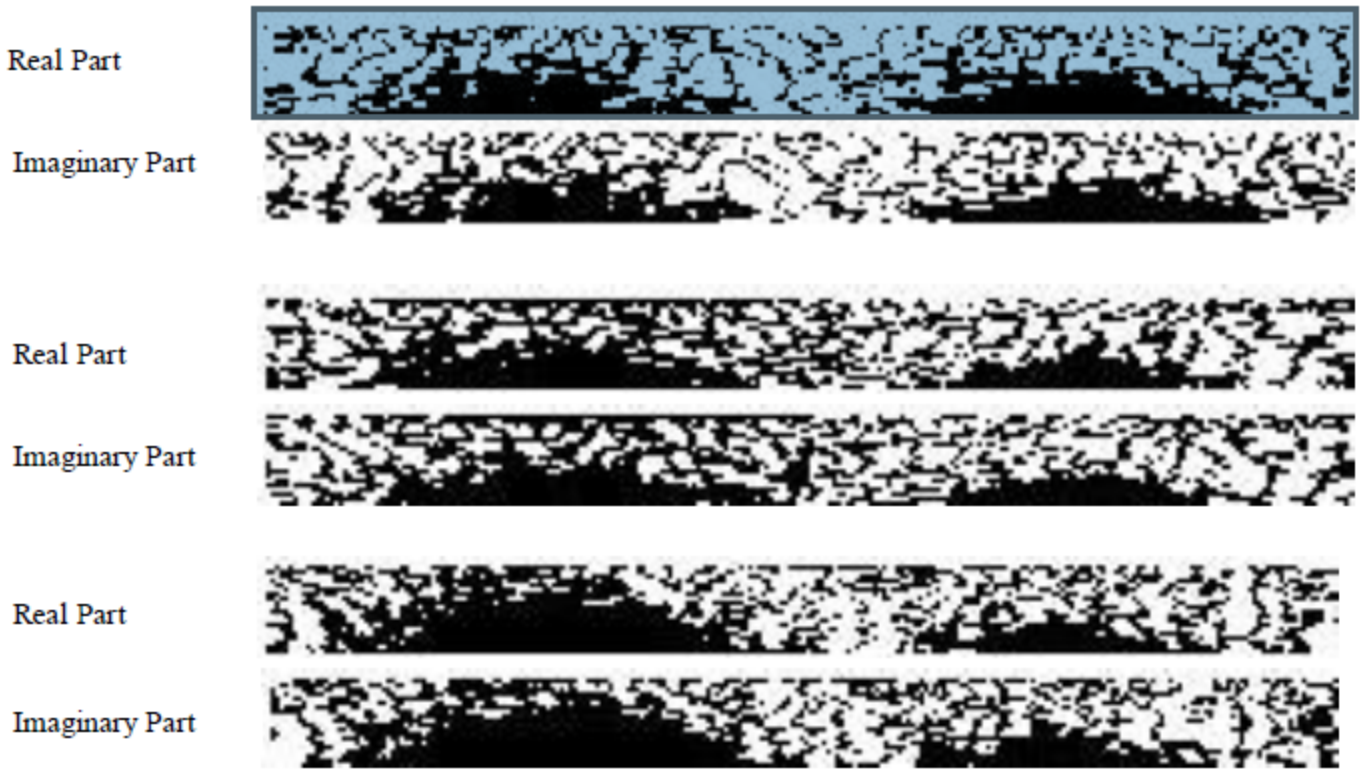

Figure 6.16: Result of comparing templates and masks for three persons.

It is found that 44.3% of the bits of iris' are consistent, while 55.7% of the bits is inconsistent or occluded by eyelashes and eyelids in dataset. This means that approximately more than the half of iris code bits are inconsistent or can be dropped or removed from the iris code. The maximum percentage of consistent bits is 64.8% and the minimum percentage equals 15.3% for one class in dataset. Due to the three cases, observed classes with low degree consistent bits:
a) If there is a small error in segmentation, because of the non-circular shape of the pupil. This lead to brittle many bits in codes of iris as shown in Figure 5.17.
b) If there is more pupil dilation range in the same person irises. This can brittle many bits in the iris' code.
c) The normal noise case like unmasked luminance, unmasked eyelashes and reflections in iris' code.

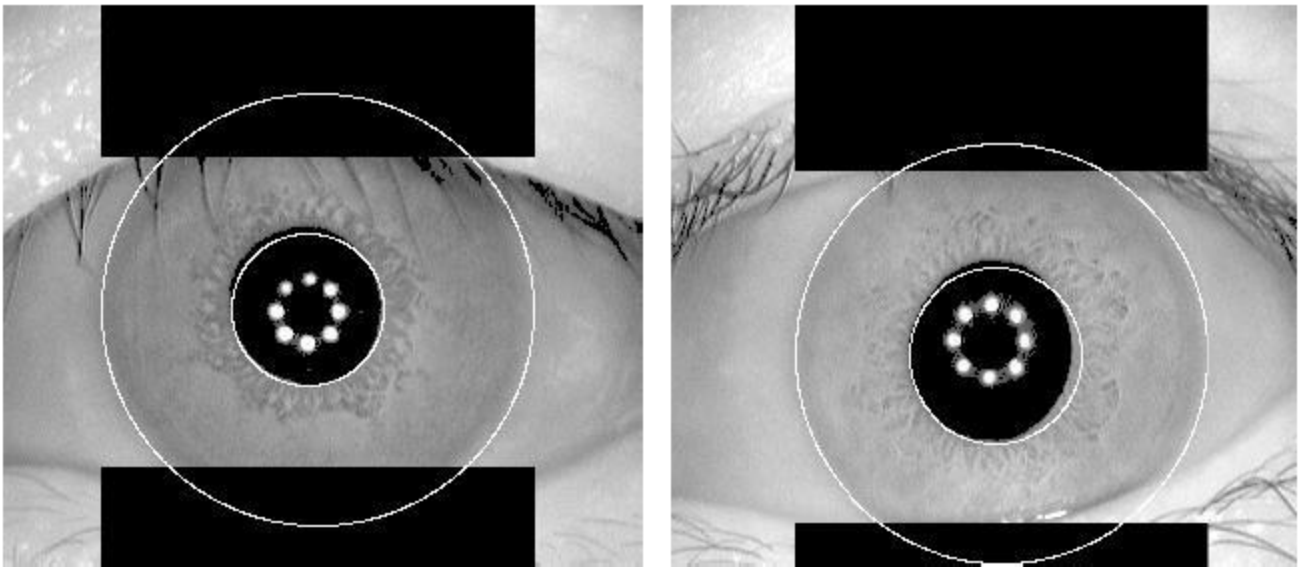

Figure 6.17: Samples of segmented irises from our selected dataset that have many inconsistent bits because the wrong segmentation due to non-circular shape of the pupil.

6.4.3 The Best Parts of Iris Code

The iris code is divided into four parts such as illustrated in Figure 6.18 to define best parts of iris code. Each part is 5x480 bits. We mask each part separately and execute the matching test as performed in the previous experiment, and we compute the FNMR for each one. Table 6.5 shows the result of masking each part separately. It is illustrated the second and third inner regions which will influence the performance when they are masked. Because when regions are masked then error rate will be a little bigger than the outer region masking.

Figure 6.18: Four parts of iris code that we use to compare the performance of each part.

The reason of this result is the many types of error which are including in two outer sectors. Because outer sector is near the pupil and might be influenced by non-

circular pupil problems and outer sector might be affected by eyelash and eyelids problems because outer sector is near the sclera.

Table 6.5: Comparison of FNMR when each of the four parts of the iris are masked.

Masked Region	FNMR
Part 1 (1-5)	0.146%
Part 2 (6-10)	0.219%
Part 3 (11-15)	0.220%
Part 4 (16-20)	0.15%

To detecting boundaries of iris and pupil, we segment all irises of the dataset using circular Hough transform and Canny edge detection to test the effect of using inner sectors on the hole system.
Through Daugman rubber sheet model using only inner two sectors segmented irises are normalized.
After that, the segmented irises are normalized using the Daugman approach. At the stage of the function coding, we convolve normalized iris patterns with 1D Log-Gabor wavelets to generate a 2x20x240 bit iris pattern for each iris. Each iris image in the database is compared with all other irises in the database to calculate the matches and nonmatches for this dataset.
Thus, the comparison groups are divided into two groups: intra-class and interclass comparisons. At the comparison stage, HD is used as a metric of uniqueness between the two considered iris codes.
FMR and FNMR errors are calculated after calculating the matches and nonmatches for this data set.
Table 6.6: Shows the comparison of results when using the two inner sectors only and when using all iris code bits.

Performance value	when using all iris code bits	when using the inner two sectors
False Match Rate	0.020%	0.019%
False Non Match Rate	0.212%	0.144%
True Match Rate	99.980%	99.981%
True Non Match Rate	99.788%	99.856 %

When using the inner two sectors of iris code in calculating the match and non-matching distributions for the datasetthe FMR and FNMR are reduced and percent of true match and true non-match are increased. Because in iris' template the inner two sectorscontain errors less than the outer two sectors and as a result iris biometric system performance will increase. When we use best parts of iris code as we see from previous table, the FNMR decreases from 0.212% to 0.144%. At the same time FMR is also decreases from 0.020% to 0.019%. This means that in the identification and authentication process we can use the inner sectors of iris template.

SUMMARY

Biometrics quickly becomes a big part of our daily life. Every time we get a new passport, a photograph is taken, the signature is used to sign important documents or scan fingerprints to unlock smartphones. The use of biometric technologies grows exponentially in order to authenticate users in such industries as state, retail and financial services.
With the increase in the number of violations of data, banks are under pressure to move away from personal identification information and toward a more impenetrable system. An inquiring conducted by the Bureau of Financial Institutions showed that 75 banks and credit union losses due to security breaches reached a total of more than $2.1 million US. This is a significant loss that financial institutions must solve in order to reduce fraud and protect users around the world.

The banks themselves do not store the caches of actual fingerprints or eyes. Rather, they create and store patterns or complex numerical sequences based on checking the fingerprint of a person or eyeball. Perhaps hackers can use a biometric template to penetrate the system. As a result, some organizations provide additional guarantees. For example, some voice authentication systems encourage the user to prove that this is a live client, not a record. Many eye checks require that users blink or move their eyes so that hackers do not use the photo for access. In addition to these guarantees, banks also need to consider multifactor authentication for an additional level of security.

REFERENCE

1.D. Zhang, ―Automated Biometrics: Technologies and Systems, Norwell, MA: Kluwer, 2000.

2. J. Daugman, ―Statistical richness of visual phase information: update on recognizing persons by iris patterns, Int. J. Comput. Vis., vol. 45, no. 1, pp. 25–38, 2001.

3. J. Daugman, ―Demodulation by complex-valued wavelets for stochastic pattern recognition, Int. J.Wavelets, Multi-Res. and Info. Processing, vol. 1, no. 1, pp. 1–17, 2003.

4. R. Wildes, ―Iris recognition: an emerging biometric technology, Proc. IEEE, vol. 85, pp. 1348–1363, Sept. 1997.

5. J. Daugman, ―How iris recognition works, IEEE Transactions on Circuits and Systems for Video Technology, 21–30 2004.

6. L. Flom and A. Safir, U.S. Patent 4 641 394, 1987. ―Iris Recognition system.

7. J. Daugman, U.S. Patent 5 291 560, 1994. ―Biometric personal identification system based on iris analysis‖.

8. J. Daugman, ―High confidence visual recognition of persons by a test of statistical independence, IEEE

Trans. Pattern Analy. Machine Intell., vol. 15, pp. 1148–1161, Nov. 1993.

9. J. Daugman, ―Demodulation by complex-valued wavelets for stochastic pattern recognition, Int. J.Wavelets, Multi-Res. and Info. Processing, vol. 1, no. 1, pp. 1– 17, 2003.

10. http://www.ey.com/Publication/vwLUAssets/ey-the-digital-bank-tech-innovations-driving-change-at-us-banks/$File/ey-the-digital-bank-tech-innovations-driving-change-at-us-banks.pdf

11. https://clearbridgemobile.com/biometric-authentication-for-mobile-banking/

12. http://wiki.gis.com/wiki/index.php/Cluster_analysis

13. http://www.ijtra.com/special-issue-view/m-banking-verification-using-otp-and-biometrics-.pdf

14. http://shodhganga.inflibnet.ac.in/bitstream/10603/77607/11/11_chapter5.pdf

15. http://biometrics.idealtest.org/dbDetailForUser.do?id=4

16. Kshamaraj Gulmire1, Sanjay Ganorkar, International Journal of Emerging Technology and Advanced Engineering ISSN 2250-2459, Volume 2, Issue 7, July 2012, Iris Recognition Using Independent Component Analysis